FINAL REPORT

(Project SR-98)

on

THE STRENGTH, ENERGY ABSORPTION AND TRANSITION TEMPERATURE OF INTERNALLY NOTCHED FLAT STEEL PLATES:

Part I Twelve Inch Wide Flat Plate Tests
  by S. T. Carpenter and W. P. Roop

Part II Aspect Ratio Program
  by S. T. Carpenter and W. P. Roop

Part III A Study of Plastic Deformation by Strain
  Energy Distribution
  by S. T. Carpenter

SWARTHMORE COLLEGE

Transmitted through

NATIONAL RESEARCH COUNCIL'S
COMMITTEE ON SHIP STEEL

Advisory to

SHIP STRUCTURE COMMITTEE

January 19, 1953

NATIONAL RESEARCH COUNCIL

2101 CONSTITUTION AVENUE, WASHINGTON 25, D. C.

COMMITTEE ON SHIP STEEL

OF THE
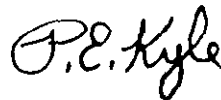
DIVISION OF ENGINEERING AND INDUSTRIAL RESEARCH

January 19, 1953

Dear Sir:

Attached is Report Serial No. SSC-47 entitled "The Strength, Energy Absorption and Transition Temperature of Internally Notched Flat Steel Plates" by Carpenter and Roop. This report has been submitted by the contractor as a Final Report on Contract NObs-45521, Bureau of Ships Project NS-011-078, between the Bureau of Ships, Department of the Navy and Swarthmore College.

The report has been reviewed and acceptance recommended by representatives of the Committee on Ship Steel, Division of Engineering and Industrial Research, NRC, in accordance with the terms of the contract between the Bureau of Ships, Department of the Navy and the National Academy of Sciences (Contract NObs-50148, BuShips Project NS-731-036).

Very truly yours,

P. E. Kyle, Chairman
Committee on Ship Steel

FINAL REPORT
(Project SR-98)

on

THE STRENGTH, ENERGY ABSORPTION, AND TRANSITION TEMPERATURE
OF INTERNALLY NOTCHED FLAT STEEL PLATES:

Part I   Twelve Inch Wide Flat Plate Tests
          by S. T. Carpenter and W. P. Roop

Part II   Aspect Ratio Program
          by S. T. Carpenter and W. P. Roop

Part III A Study of Plastic Deformation by Strain
          Energy Distribution
          by S. T. Carpenter

SWARTHMORE COLLEGE
under
Department of the Navy
Bureau of Ships
Contract NObs-45521
BuShips Project No. NS-011-043

SHIP STRUCTURE COMMITTEE

TABLE OF CONTENTS

Table of Contents (continued)

LIST OF FIGURES

Part I

iii

LIST OF FIGURES

Part II

iv

LIST OF FIGURES

Part III

LIST OF TABLES

Part I

List of Tables (Cont'd)

Part II

ABSTRACT

This is a final report presenting the results of an extended series of tests made mainly to determine the effects of temperature upon strength, energy absorption and transition temperature of ship plate steels in tension specimens of "wide plate" type with standardized internal notches.

The report is presented in three parts, the first part dealing with 12" wide by 3/4" thick specimens. Most of the steels used were the so-called pedigreed steels.

The second part of the report deals with geometrically similar internally notched steel plates of variable width and thickness. The objective of these tests was to separately determine the metallurgical and geometrical effects of plate thickness. All plates were tested in "as rolled" thickness.

The third part of the report concerns detailed studies to determine the energy distribution in 12" wide internally notched plates. Unit strain energy was computed using surface strains obtained by grid measurements.

The program reported in this paper was sponsored by the Ship Structure Committee and was conducted through a Bureau of Ships Contract and coordinated by the Committee on Ship Steel of the National Research Council.

ix

FINAL REPORT

GENERAL INTRODUCTION

This is a summary report based on earlier Progress Reports [1], (2), (3), (4)* (Ship Structure Committee reports SSC-21, SSC-35, SSC-44, SSC-38) bearing on the general subject of the effect of temperature on the plastic behavior of ship plate steel.

This final report is presented in three parts to clarify and summarize the objectives and the findings of the separate phases of the project which followed different approaches. The observations of the separate phases are presented in three parts as follows:

    Part I   Tensile tests of 12 inch wide internally notched
               flat plate specimens, 3/4 inch thick.

    Part II   Aspect Ratio Program. Tensile tests of internally
               notched plates of varying width and thickness.

    Part III   Studies of Energy Distribution in 12 inch wide
               plates.

Part I and Report No. SSC-21[1] were concerned with the "Pedigreed Steels" previously studied by the University of California[5] and the University of Illinois[6]. The "Pedigreed Steels" has also been used in many other investigations, and for correlation purposes it was desirable to extend the original data by additional tests under identical conditions.

---

*Superscripts refer to references listed in Bibliography.

Tests on 12" wide notched plates were also made on a series of samples termed the "S" Steels, intended to show the effect of certain chemical, metallurgical and rolling mill practices. This laboratory has investigated three steels from this series, and the David Taylor Model Basin[7] has reported on five of the "S" Steels. In addition, this laboratory investigated "W" Steel. These results were presented in Report No. SSC-35[2].

Part II describes the investigations of metallurgical and geometrical effects on strength, energy absorption and transition temperature. This part of the project has been termed the "Aspect Ratio Program." Plates rolled from one heat of steel in thicknesses of 1/2", 3/4", 1" and 1½" were used in preparing geometrically similar internally notched tensile specimens. This approach to the problem contemplated a segregation of the metallurgical effects and geometrical effects. This part of the investigation has been reported in detail in Report No. SSC-44.[3]

Part III deals with an exploratory study of the strain energy absorption patterns in 12" wide internally notched specimens. Strain energy was computed from strains obtained by grid measurements. Specimens were strained at two temperatures, at which fracture occurred in the shear and cleavage modes. The purpose of the study was to determine the difference by which plates absorbed energy in the two modes of fracturing. A second purpose of the study was to explore the possibility of an extrapolation

of the results obtained from narrow specimens to wide specimens. The details of this study were reported in Report No. SSC-38.[4]

PART I

by

S. T. Carpenter and W. P. Roop

TWELVE INCH WIDE FLAT PLATE TESTS

INTRODUCTION

The tests[1], [2] reported herein were made on internally notched 12" wide by 24" long steel plates in their as-rolled thicknesses, (nominally 3/4" thick). The steels tested bore the code symbols "A", "C", "Bn", "Br", "Dn", "E", "W", S-9, S-12 and S-22. The first six steels have been commonly referred to as "Pedigreed Steels" and have been used in many other investigations. The "S" Steels were part of a program involving steels S-1 to S-23 inclusive, with David Taylor Model Basin[7] testing and reporting on S-1 to S-5 inclusive.

The primary objective of testing the "Pedigreed Steels" was to supplement the data previously obtained by the University of California[5] and the University of Illinois[6] on these steels. These had come to be regarded as steels upon which certain important correlation studies could be based. Another objective was to ascertain the effect of distance of the specimen from the edge of the rolled plate upon transition temperature and energy absorption. The "S" Steels were introduced into the program mainly to determine the difference with respect to cold brittleness between fine grained and coarse grained steels.

MATERIALS

The chemical analyses and physical properties of the plates
are given in Tables 1 and 2.*

The "S-9" steel had a mill designation of Type ASTM A7-46.
The "S-12" and "S-22" steels were both from the same heat where
"S-12" and "S-22" steels were both from the same heat where "S-12"
was fine grained since aluminum had been added in both the ladle
and the mold, while "S-22" was coarse grained in that aluminum
had been added in the ladle only.

TEST SPECIMENS AND TESTING TECHNIQUES

Test Specimens

Figure 1 represents a 12" wide x 24" long internally notched
plate specimen, with the 24" dimension in the direction of rolling
and of the applied tensile loading. The length of the central
slot is 3" (one-quarter of the width) and terminates with a
jeweler's hacksaw cut, about 0.010" wide.

The test specimens were flame cut from larger plates and then
machined to exact width. The plate layout showing the position
of the specimens is given in Figure 2 for the 6' x 10' plates and
in Figure 3 for the 6' x 6' plates. Test specimens are identified
by the code letter of the steel, followed by a laboratory serial
number, and the last number gives the location of the specimen
within the plate according to the layouts shown in Figures 2 and 3.
For example, A-18-13 identifies a specimen of "A" steel, but from

*All tables at end of report, beginning on page

-6-

12"

6"   6"

3"

24"±

$\frac{3}{4}$ ∅ REAMED

STD. HACK
SAWCUT

$1\frac{1}{2}$" $1\frac{1}{2}$"

$\frac{3}{4}$"
A

$\frac{1}{8}$"   JEWELER'S SAWCUT .010" $\frac{1}{8}$"
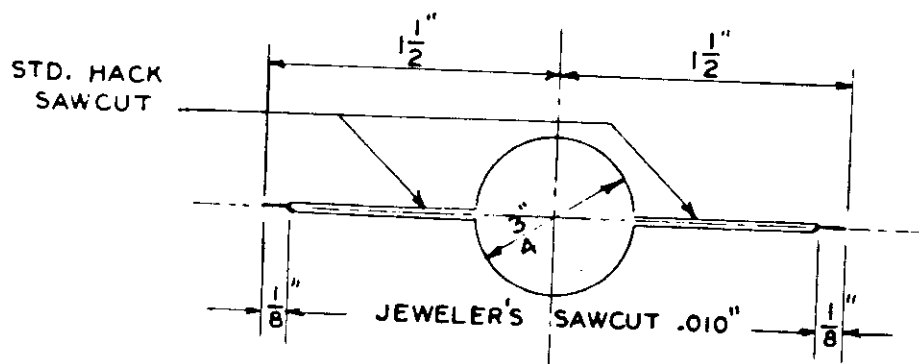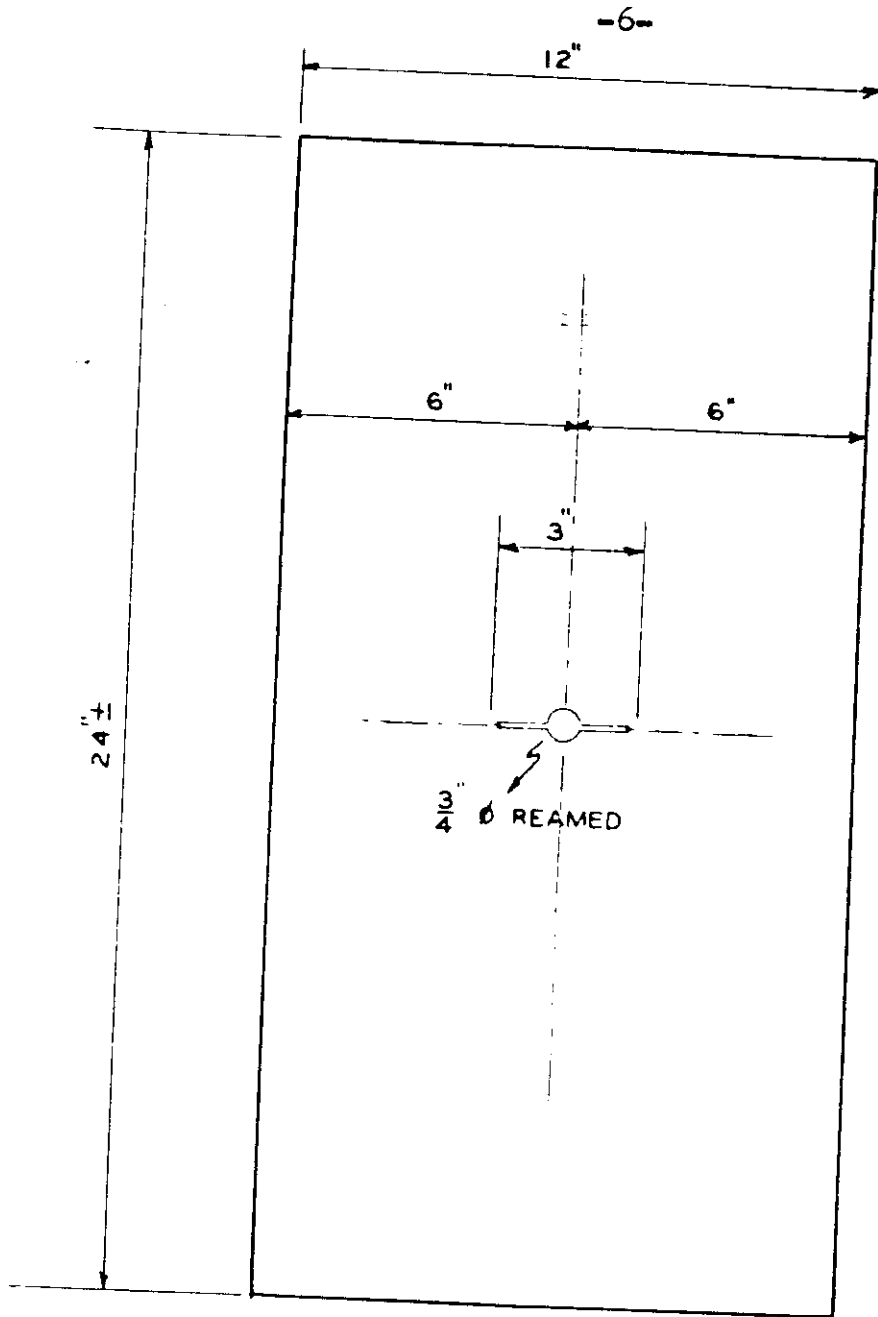
FIG. I
NOTCH LAYOUT
SWARTHMORE COLLEGE
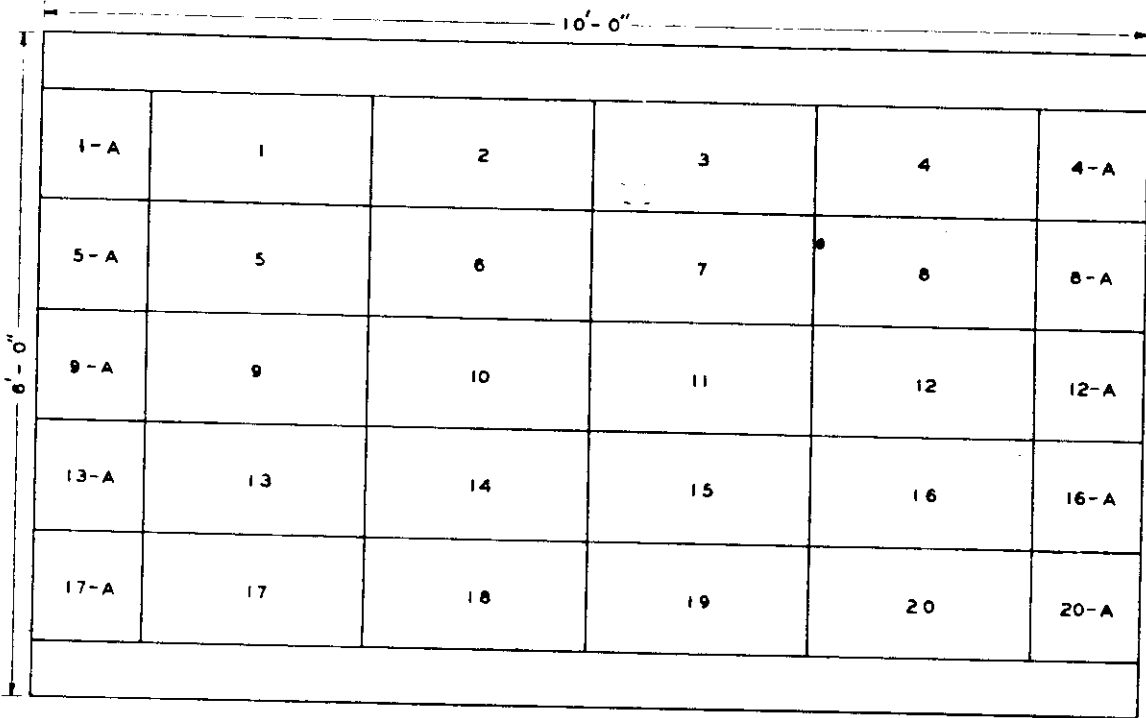
ALL SPECIMENS 12"WIDE X 24"LONG

FIG. 2   TYPICAL 6'X 10' PLATE LAYOUT – LOCATION OF SPECIMENS
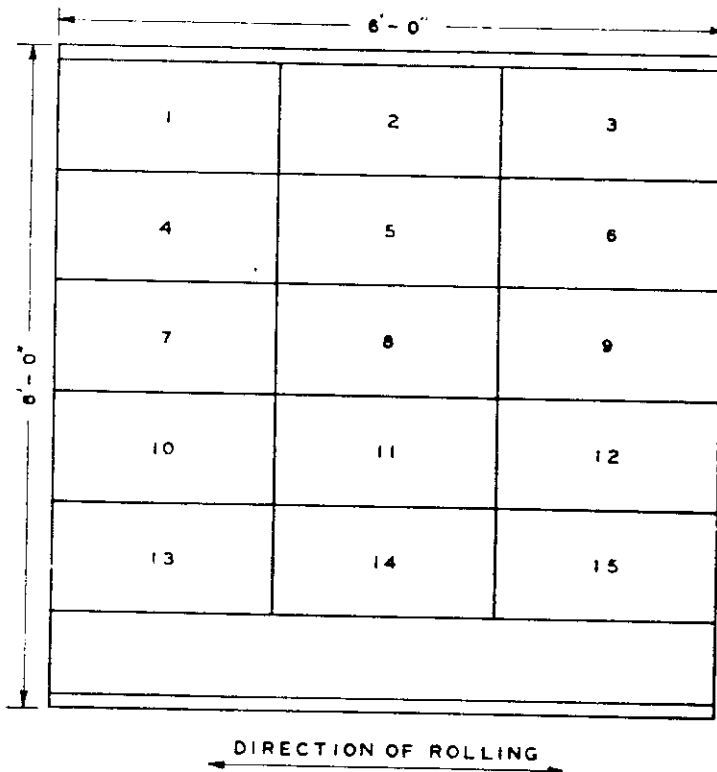
ALL SPECIMENS 12"WIDE X 24"LONG

FIG.3   TYPICAL 6'X 6' PLATE LAYOUT – LOCATION OF SPECIMENS

SWARTHMORE COLLEGE

plate Number 18, specimen location being No. 13.

All specimens were butt-welded to $1\frac{1}{4}$" thick pulling heads, which were gripped by the jaws of a 600,000 lb. testing machine. Preparation of the test specimens is fully described in previous reports [1], [2].

Measurement of Elongation

Elongations were measured over a gage length of 9" (three quarters of the width of the plate), symmetrical with the notch, at five stations on each face of the plate, and one on each edge. 12 slip gages were used with bakelite-bonded SR-4 pick-ups. The mounting of each gage was such as to permit individual elongation readings.

Figure 4 shows the complete setup of gages on a test specimen and further details may be found in a previous report[1].

Temperature Control

A transparent temperature control chamber surrounded the specimen. The chamber was either cooled by air blown over dry ice, or warmed by heating with electric strip heaters. The temperature of the specimen was obtained by using thermocouples placed near the ends of the notch. See previous report[1] for full details.

Testing Procedure

The tensile loading of the specimen was applied in successive
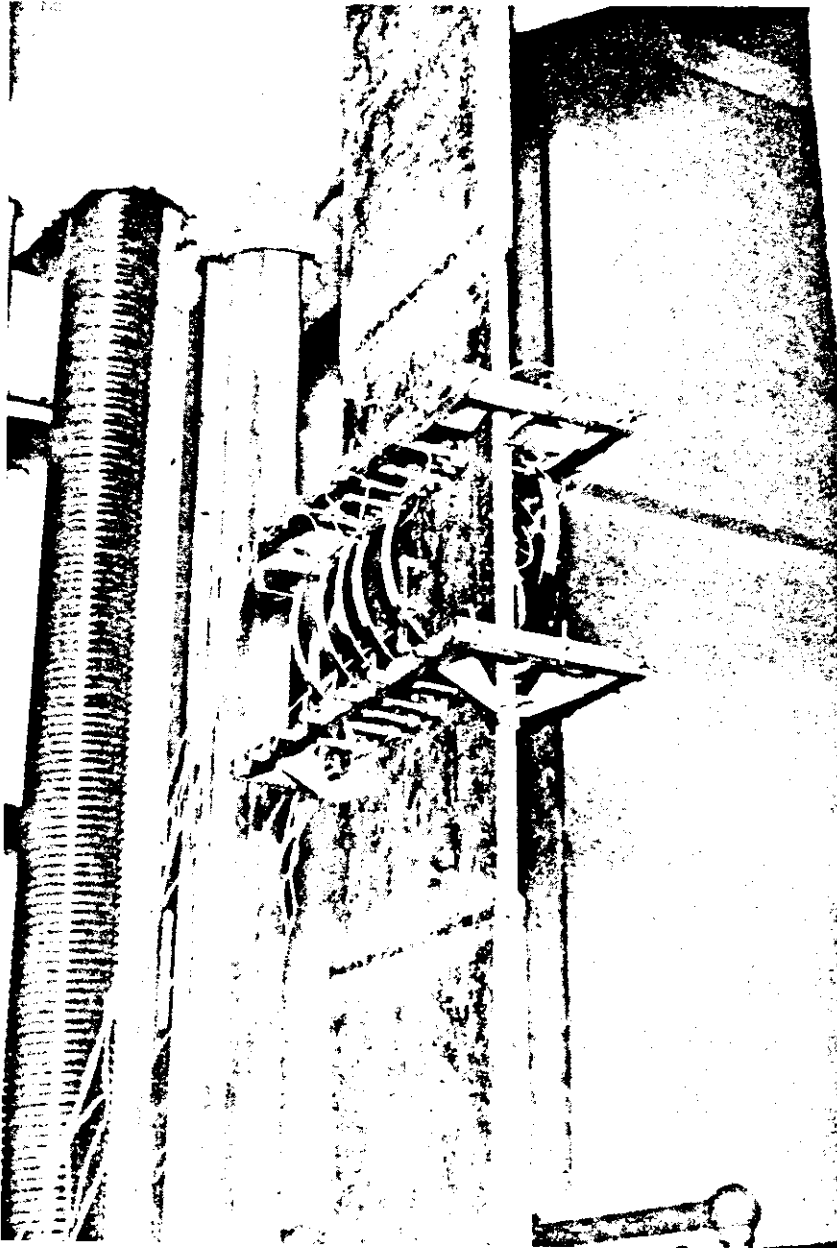
Figure 4. Specimen with strain gages

increments sufficient to produce approximately equal steps of
elongation. At each reading the pump loading was stopped and
the load value drifted downward a little. The value plotted
was that prior to drift. Extremely low strain rates were in-
volved; approximately 45 minutes elapsed from the zero load to
the maximum load for all specimens.

TEST RESULTS

Data

Tables 3 to 12 inclusive list the basic data, while Figures
5 to 14 inclusive give a graphical summary of the data for each
steel. The important quantities in the tables for each specimen
are the testing temperature, the loads, energy input, and char-
acter of the fracture, as defined by the percent of shear failure
in the fracture. Significant values of load recorded in the
tables are: (a) Load to produce the visible crack at the base
of the notch, (b) the maximum load, and (c) the last observable
load, noted as the failure load, at the moment of complete se-
paration of the specimen. The energy inputs to these three
separate load stages were computed by taking areas under the
plotted load-elongation curve and are denoted in this report as

E - Energy to visible crack loading

E_1 - Energy to maximum load

E_2 - Energy to failure load

MAX. LOAD VS. TEMP.

ENERGY TO MAX. LOAD VS. TEMP.

PERCENT SHEAR VS. TEMP.
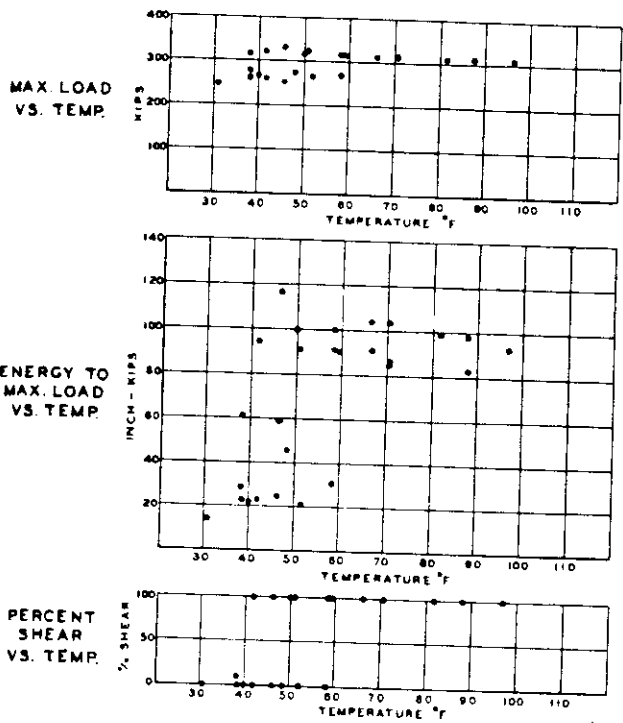
12" x ¾" x 24" SPECIMENS
SEE TABLE FOR DATA

FIG. 5   A - STEEL
         SUMMARY

MAX. LOAD VS. TEMP.

ENERGY TO MAX. LOAD VS. TEMP.

PERCENT SHEAR VS. TEMP.
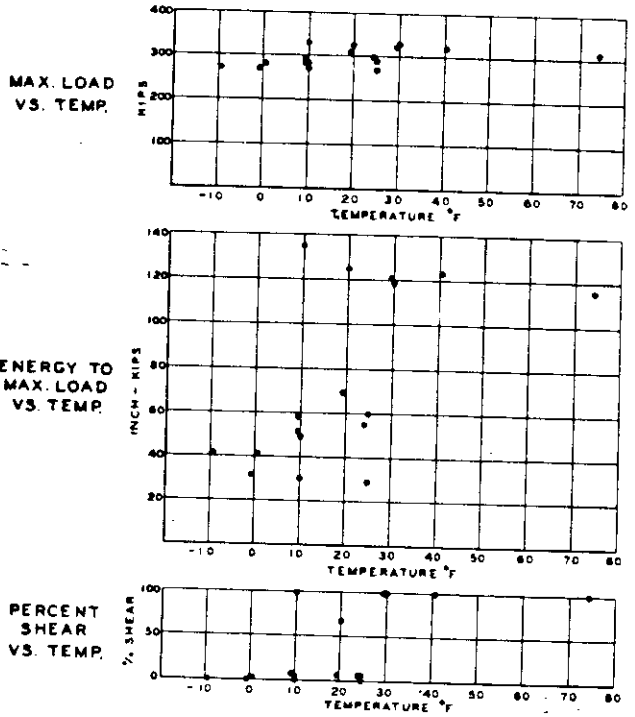
12" x ¾" x 24" SPECIMENS
SEE TABLE FOR DATA

FIG. 6   BN - STEEL
         SUMMARY

MAX. LOAD VS. TEMP.

ENERGY TO MAX. LOAD VS. TEMP.

PERCENT SHEAR VS. TEMP.
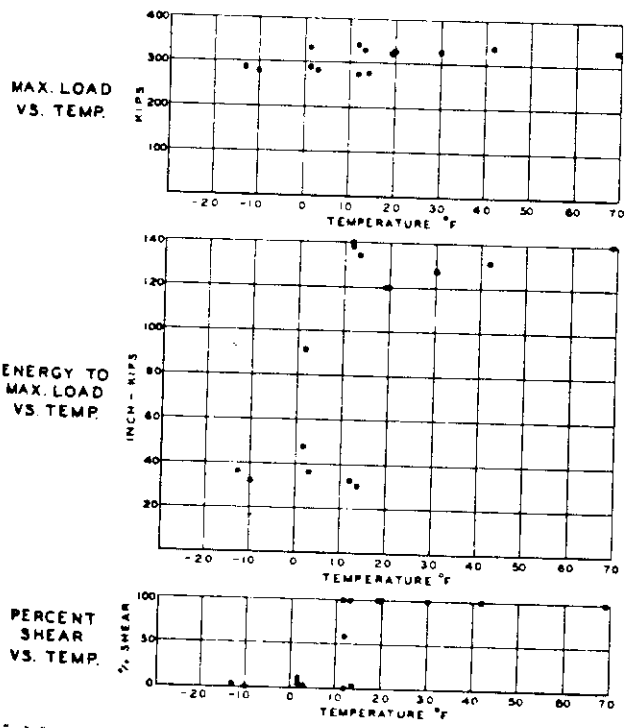
12" x ¾" x 24" SPECIMENS
SEE TABLE FOR DATA

FIG. 7   BR - STEEL
         SUMMARY

MAX. LOAD VS. TEMP.

ENERGY TO MAX. LOAD VS. TEMP.

PERCENT SHEAR VS. TEMP.
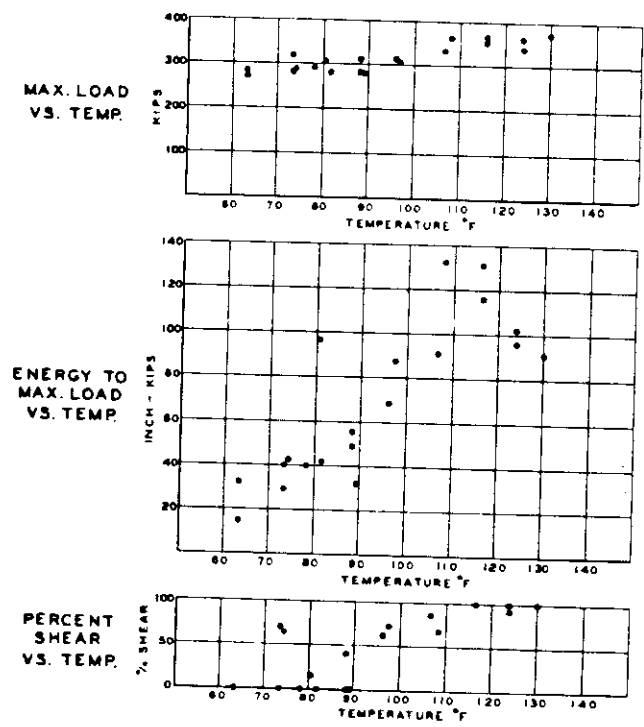
12" x ¾" x 24" SPECIMENS
SEE TABLE FOR DATA

FIG. 8   C - STEEL
         SUMMARY

-12-
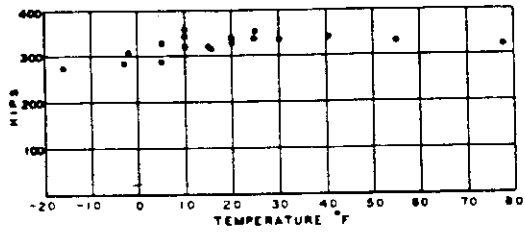
MAX. LOAD
VS. TEMP.

ENERGY TO
MAX. LOAD
VS. TEMP.
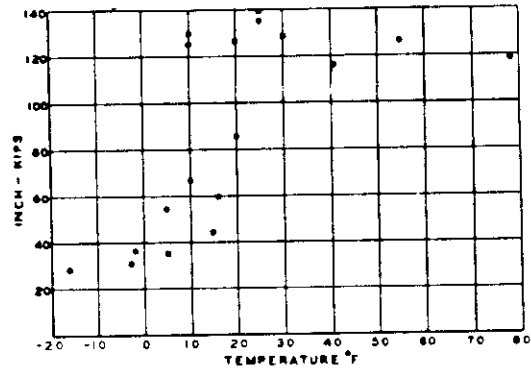
PERCENT
SHEAR
VS. TEMP.
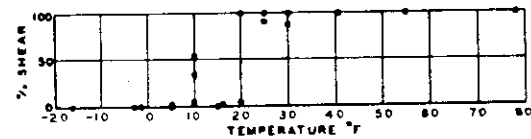
12" x 3/4" x 24" SPECIMENS
SEE TABLE FOR DATA

FIG. 9   DN - STEEL
SUMMARY

MAX. LOAD
VS. TEMP.
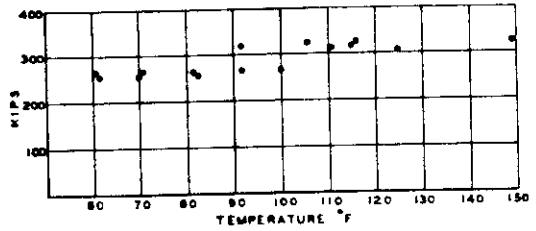
ENERGY TO
MAX. LOAD
VS. TEMP.
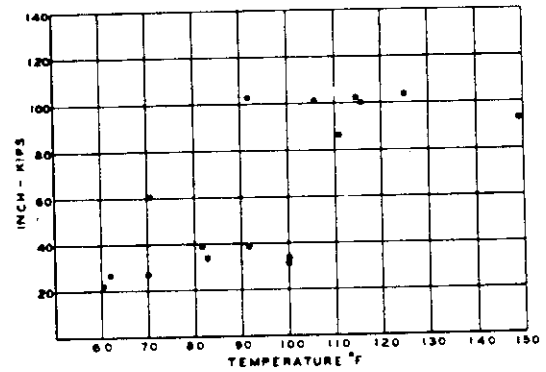
PERCENT
SHEAR
VS. TEMP.
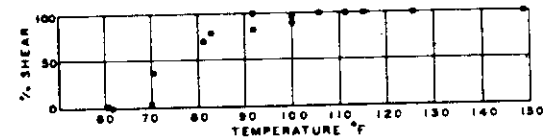
12" x 3/4" x 24" SPECIMENS
SEE TABLE FOR DATA

FIG. 10   E - STEEL
SUMMARY

MAX. LOAD
VS. TEMP.
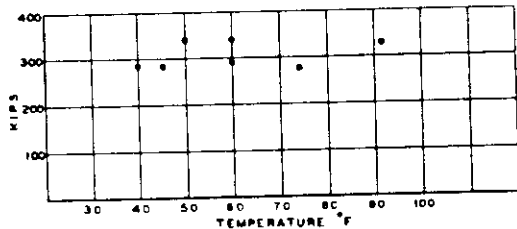
ENERGY TO
MAX. LOAD
VS. TEMP.
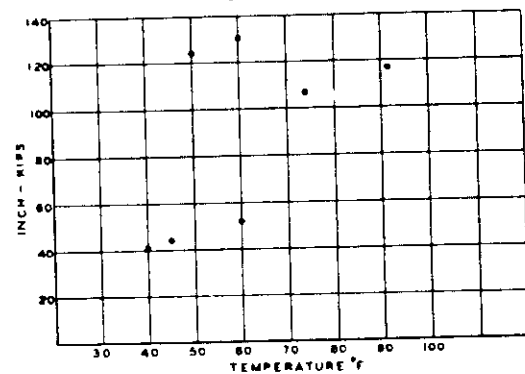
PERCENT
SHEAR
VS. TEMP.
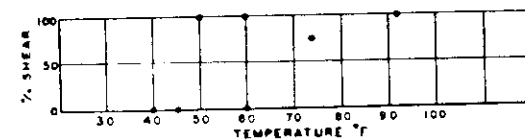
12" x 3/4" x 24" SPECIMENS
SEE TABLE FOR DATA

FIG. 11   S9 - STEEL
SUMMARY

MAX. LOAD
VS. TEMP.
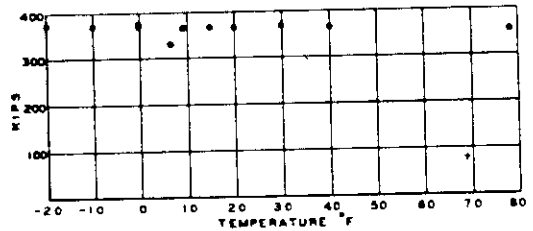
ENERGY TO
MAX. LOAD
VS. TEMP.
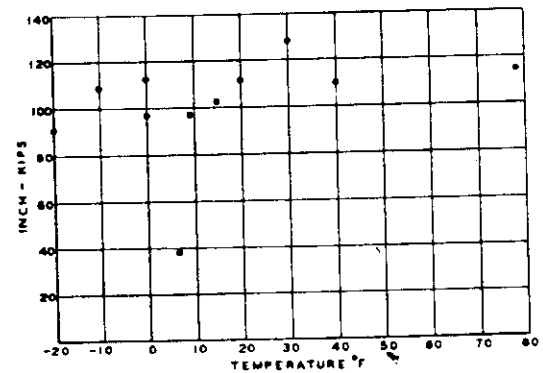
PERCENT
SHEAR
VS. TEMP.
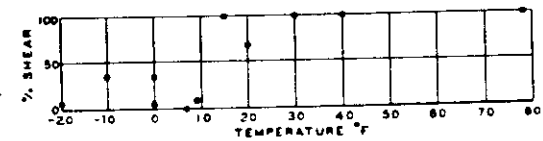
12" x 3/4" x 24" SPECIMENS
SEE TABLE FOR DATA

FIG. 12   S12 - STEEL
SUMMARY
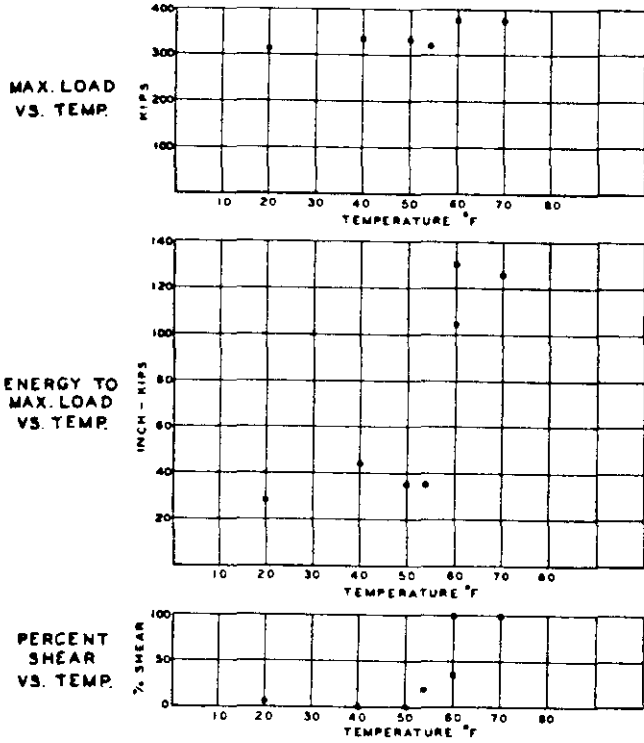
MAX. LOAD VS. TEMP.

ENERGY TO MAX. LOAD VS. TEMP.

PERCENT SHEAR VS. TEMP.

12" x 3/4" x 24" SPECIMENS
SEE TABLE FOR DATA

FIG. 13 S22-STEEL
SUMMARY

MAX. LOAD VS. TEMP.

ENERGY TO MAX. LOAD VS. TEMP.

PERCENT SHEAR VS. TEMP.
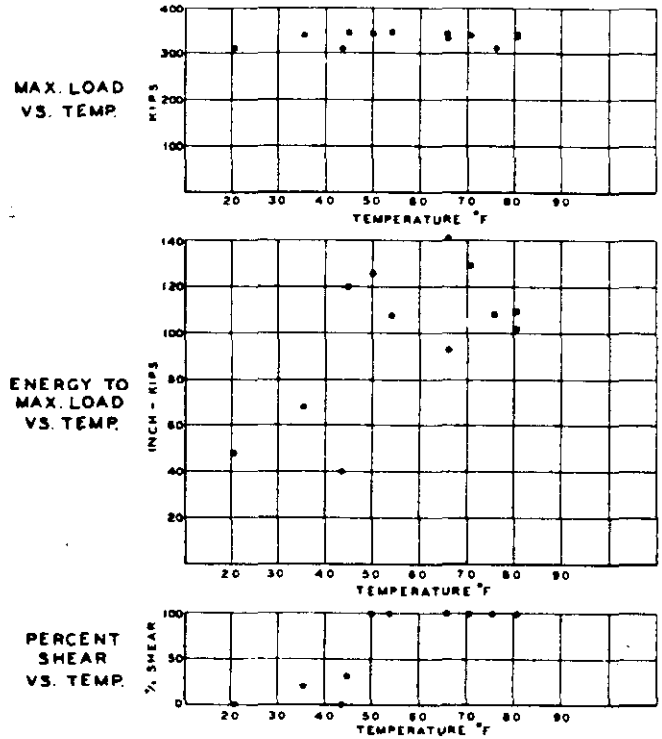
12" x 3/4" x 24" SPECIMENS
SEE TABLE FOR DATA

FIG. 14 W- STEEL
SUMMARY

MAX LOAD 324,800 LBS.

VIS CRACK 235,500 LBS.

ENERGY TO VIS CRACK 4,900 IN LBS.
ENERGY TO MAX LOAD 110,000 IN.LBS.
ENERGY TO FRACTURE 290,000 IN.LBS.

FRACTURE 40,000 LBS.
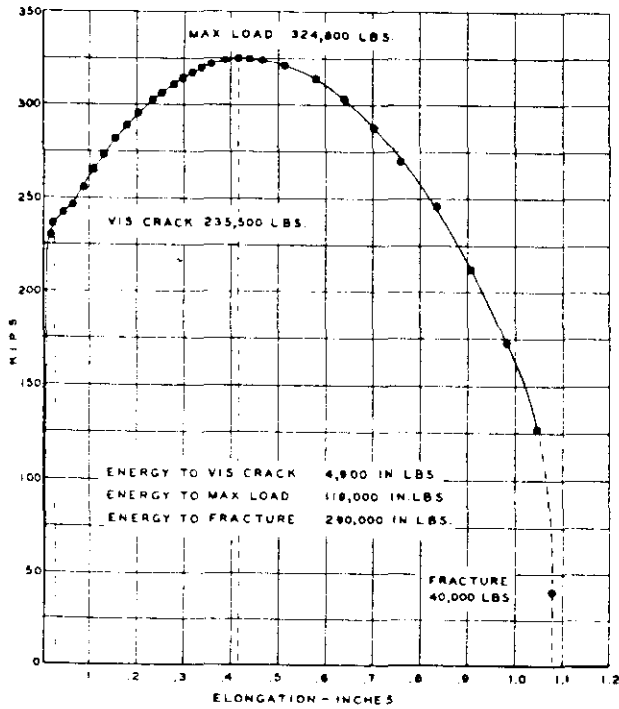
FIG. 15 LOAD-ELONGATION CURVE
SPECIMEN BN 21-20 (30°F,100% SHEAR)

MAX. LOAD FRACTURE 270,800 LBS.

VIS. CRACK 240,000 LBS.

ENERGY TO VIS CRACK 7,700 IN.LBS
ENERGY TO MAX. LOAD
ENERGY TO FRACTURE }32,900 IN.LBS.
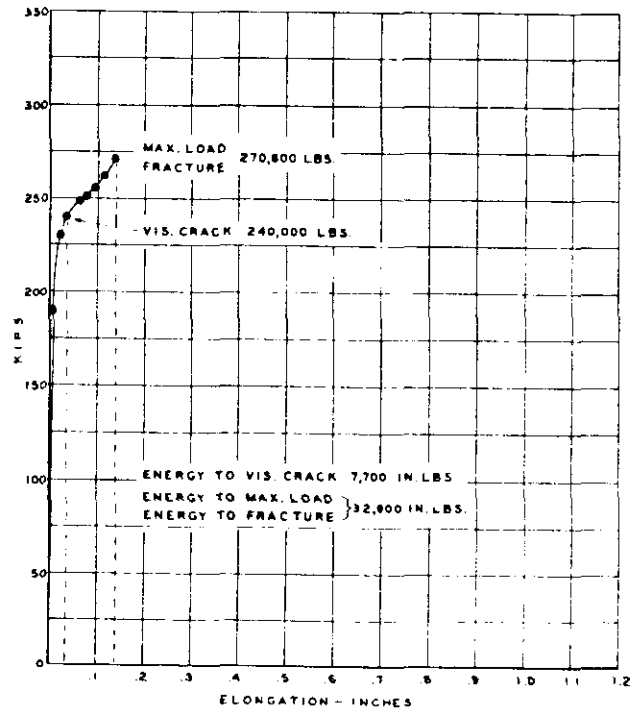
FIG. 16 LOAD-ELONGATION CURVE
SPECIMEN BN 21-1 (1°F, 0% SHEAR)

In the case of a complete cleavage failure $E_1 = E_2$. Figures 15 and 16 show the typical form of the load-elongation curves for a shear and cleavage failure respectively for "Bn" steel. Load - elongation diagrams for all specimens tested in the Part I program have been given in Progress Reports [1], [2].

DISCUSSION OF TEST RESULTS

Fracturing Characteristics

During all tests the first visible crack at the root of the notch was observed at mid-thickness of the plate. This initial crack grew in depth and extended to the faces of the plate with greater applied load. X-ray studies made of the progress of the crack front with increasing load indicate that the crack had penetrated about 1/2" in depth at the plate mid-thickness before the crack front reached the surfaces of the plate. The crack front, after extending to the surfaces, became bell shaped.

Through plastic flow of the metal in this stage the initial acuity of the jeweler's hack saw cut was destroyed and a new acuity was created.

The main features of this preliminary stage were the same whether the final rupture was by shear or cleavage. In a specimen failing in cleavage the visible crack occurred at approximately the same load as for a ductile specimen but perhaps did not extend as far in depth before failure. It has been impossible to ascertain whether this initial crack is the result of a cleavage

or shear failure. However, a new notch (the crack front) was definitely present in all specimens before fracture. The acuity at the moment of choice between advance to rupture by shear or by cleavage was always that of a natural crack.

Specimens failing in shear fractured either along a single 45° shearing plane or along two such planes. The former case was more prevalent but the latter type occurred most often in the transition zone. Specimens failing in cleavage would generally separate completely upon reaching the maximum load; but the photographs of the fractures [1], [2] indicate that variations of this occurred. One variation was an initial failure by cleavage after which the crack halted at some distance from the notch. (See Figure 23 of Ref. (1)). Further loading might then either produce a second cleavage jump or the mode of rupture might change into shear.

The character of the fracture surfaces could usually be rated "granular" or "fibrous" for all pedigreed steels except "Br and "Bn." An exception is noted for a number of "Br" specimens where the fracture surface had a sandwich appearance as shown in Figure 17 with approximately three equal and distinct zones (striation) the center zone having the coarser texture.

Of the steels tested, the fracture surfaces of steels "C" and "E" were the most variable, exhibiting a mixture of cleavage and shear fracture surfaces over a wide range of temperature. Specimen

E-36-2, Figure 18, is of interest because the specimen appeared to fail "instantaneously" in cleavage, although examination of the fracture shows that the crack front paused and then continued to fracture.

The cleavage fractures of "S-12" and "S-22" steels differed in appearance; the fractures for "S-12" were extremely rough and ragged in comparisons to the fracture surfaces of the "S-22" steels. Also the energy to maximum load for S-12 did not fall away at low temperature, and this may possibly be related to the unusual appearance of the fracture.

Several specimens of "Bn" and "E" steels, (see previous Reports[1],[2]) exhibited what may be termed a first and second maximum load. This second maximum load occurred after an initial partial cleavage fracture at the first maximum load. In some instances considerable elongation was noted in reaching the second maximum load after which fracture might be completed either by cleavage or shear.

Effect of Mode of Fracture on Loads

A comparison of maximum loads in cleavage and shear is shown in Table 13. The ratio of loads for the two modes is quite consistent but maximum loads do not correlate with the tensile properties of the steels as determined by A.S.T.M. unnotched tensile tests. Maximum stress over net initial area in the shear mode varies from 47,000 psi to 56,000 psi, and in the cleavage mode
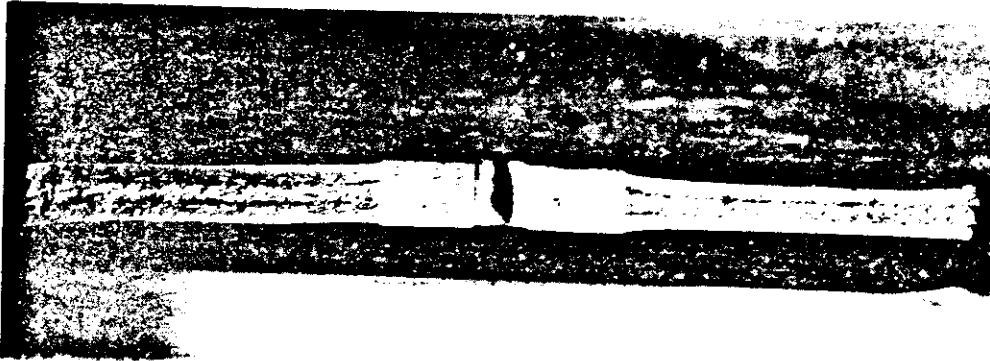
Fig. 17. Fracture Surface of a "Br" Specimen
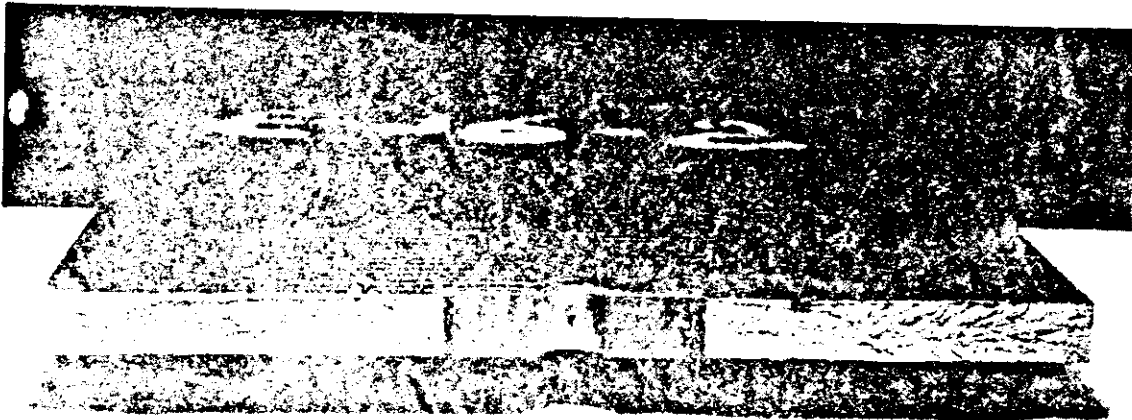
Fig. 18. Fracture Surface of Specimen E-36-2

from 40,000 psi to 49,000 psi. Thus shear and cleavage failures were induced by average stresses somewhat above yield stresses but below ultimate values, as determined from standard tensile tests, indicating that even in a relatively simple structure such as the present notched specimen, the strength of the specimens bears no clear cut relation to the tensile properties of the material as found in unnotched specimens.

As the crack slowly advances in a ductile specimen, the applied loads do not fall off with the net cross-sectional area. As an example of this, for specimen A-18-9, a load of 286,000 lbs. initiated the tearing of specimen at the notch, with an average longitudinal tensile stress of 43,100 psi. At the maximum load of 314,500 lbs., the tearing at the notch left a net width of 7 11/16", giving an average tensile stress on the net area of 52,000 psi. Additional stretching of the specimen increased the length of crack until at a load of 198,000 lbs. the average unit stress was 75,400 psi. The last observable load for this specimen was 133,500 lbs. with only 7/8" of the original width intact, giving an average tensile stress of 237,100 psi. This action is common for all ductile specimens and may be explained by the strain hardening action induced by the large strains in the fracture zone of the plate prior to failure. High local stress values at the apex of the advancing crack are accompanied by high rates of energy absorption there (See Part III).

Effect of Mode of Fracture on Energy

A comparison of energy absorbed to maximum load for the cleavage and shear modes of failure is shown in Table 14. The ratios of the energies at maximum load in the shear mode to those in cleavage mode are much more variable than the maximum load ratios. If it should be supposed that the energy in the cleavage mode is important to a designer, then steel "A" would appear to be inferior. However, such a conclusion would be difficult to accept. The role of capacity for energy absorption in deciding the suitability of a steel for structural use can be evaluated only after a more complete analysis of the data.

Transition Temperature

The transition temperature for a given steel depends upon the form of the test specimen and the quantity whose variation with temperature is observed. Various quantities such as loss of thickness, bend-angle, energy, fracture appearance, and strength, as they have varied with temperature, have been used to define the transition temperature. It has been the usual practice to name a single value of transition temperature notwithstanding the scattering of data in the transition zone. This laboratory prefers to state the transition temperature in terms of a temperature range rather than of a single value, where the upper limit of the range indicates that temperature below which one can not be sure of fully ductile action. The lower limit of the temperature range indicates that temperature below which it is expected

that no mixed fractures of shear and cleavage will occur. For correlation purposes, however, this report gives both a range and a single value considered suitable for comparison with transition temperatures based on half-value, as determined by other investigators.

Transition temperatures of this report are based on energy to maximum load as well as on appearance of the fracture. No use has been made of the data on energy absorbed beyond maximum load. Transition temperature range is determined by an inspection of the data to ascertain the range of temperature through which the absorbed energy or the fracture appearance indicates a chance of embrittlement. A single transition temperature based either on energy or appearance has been selected by drawing an average curve representative of the data and selecting the temperature at which the energy or percent of shear is midway between their respective maximum and minimum values. This latter method could give the same results for two steels even though the upper limit of the transition zone for one might be much higher than for the other.* It is believed that the transition temperature range better expresses the difference between such steels, and the upper limit of the stated range provides an important index to the steels' initial susceptibility to embrittlement.

---

*In a few cases it led to the anomaly of a single value lying outside the range of values.

Table 15 summarizes the transition temperature ranges, and the single values of transition temperature for all steels tested, along with the values determined by the Navy Tear Test[8],[9]. The results obtained at the University of California[5] and the University of Illinois[6] are also given. Energy to maximum load and appearance indicate the same temperature range with only two exceptions, steels C and S-12. The single temperature values based on energy to maximum load and on appearance are also quite close to each other.

For "Br" and "S-12" reduction of thickness at the base of the notch seems to diminish at the transition temperature as determined from energy and appearance (See Figures 19, 20.)

A diagram of correlation of the present results with those of the Navy Tear Test is given in Figure 21. The correlation based on transition range indicates that ΔT , the transition temperature differential between results obtained by the Tear Test and by the 12" wide plate test, may be between $+10^{\circ}$ and $+52^{\circ}F$ with a median value of $+31^{\circ}F$. The Tear Test value is always higher. This may be compared with a ΔT of $+40^{\circ}F$ found by MacCutcheon, Pittiglio and Raring[7] for other mild steels. The California and Illinois transition temperatures correlate reasonably well with the Swarthmore values. The Swarthmore data place the transition of "A" steel 17° higher end of the "Bn" steel 11° higher than these previously reported values.

THICKNESS REDUCTION AT ROOT OF NOTCH
IN PER CENT

THICKNESS REDUCTION AT ROOT OF NOTCH
IN PER CENT

FIG. 20 THICKNESS REDUCTION AT ROOT OF
NOTCH FOR SI2 STEEL.

FIG. 19 THICKNESS REDUCTION AT ROOT OF
NOTCH FOR BR STEEL.

o SHEAR FAILURE
● CLEAVAGE FAILURE
◉ PARTIAL SHEAR-CLEAVAGE
    FAILURE

TEMPERATURE °F

-22-
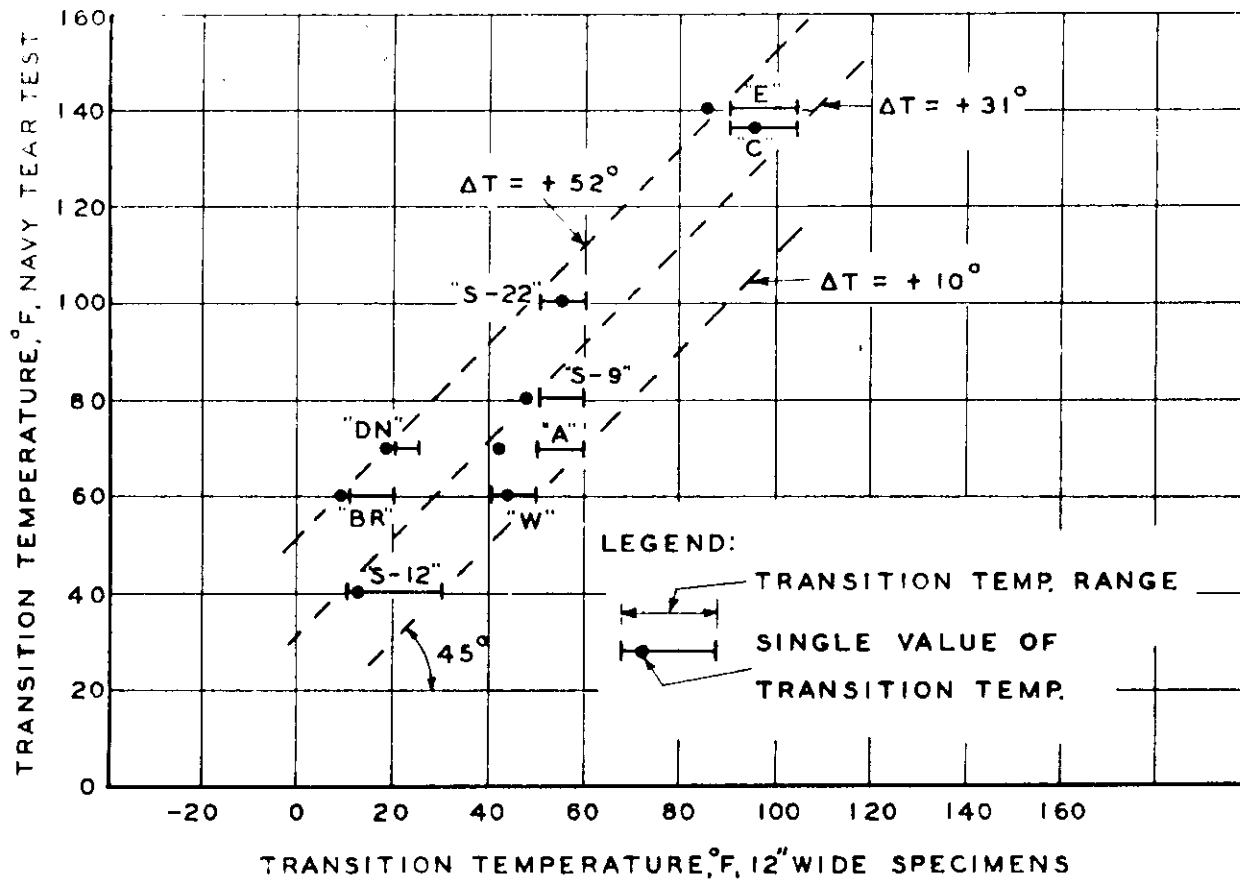
FIG. 21   CORRELATION OF TRANSITION TEMPERATURE
12"WIDE SPECIMENS VS. NAVY TEAR TEST.

The other steels agree more closely. It appears that by increasing the number of tests a narrower range of transition has been determined.

Variations due to Location of the Specimen within a 6' x 10' plate

The tests were planned in part to bring out differences due to location within the rolled plate. On an energy basis it is common for specimens from the outside zones at the rolled edges of the plate, when compared with specimens from the center zone (ap approximately the same temperature), to show less variation than that between specimens in the center zone. Aside from this, the results do not warrant the making of any general statements.

Effect of Manganese-Carbon Ratio

High ratio of manganese to carbon has been said to be a cure for cold-brittleness. In the present data the agreeement of the transition temperature with the order of the Mn/C ratio, where carbon content is essentially constant, is shown in Table 16. "S-22" has a transition temperature 30° to 40° higher than for "S-12" with identical Mn/C ratio; the coarse grain in "S-22" compared with the fine grain of "S-12" was the controlling influence. It appears that the data of this report are too limited to warrant any conclusions being drawn concerning the Mn/C ratio and grain size effect. Normalizing in the case of

of "Bn" compared with "Br" did not materially change the transition temperature, "Bn" having transition higher than "Br" by a small margin.

CONCLUSIONS - PART I

1.) The internally notched flat plate specimens taken as representing a ship's deck plating, show temperature effects similar to those occurring in service.

2.) Before direct inference can be made about safety of a given steel in service, the difference between the laboratory specimen and the service structure must be more completely understood.

3.) The results of these tests confirm those of earlier work with the same type of specimen, particularly as to high transition temperature for "C" and "E" steels.

4.) The 12" wide by 3/4" thick internally notched flat plate tests determine the transition temperature at about $30^{\circ}F$ lower than the Navy Tear Test.

PART II

by

S. T. Carpenter and W. P. Roop

ASPECT RATIO PROGRAM

INTRODUCTION

This is an exploratory investigation of the effects of specimen geometry (width and thickness) on strength, energy absorption and transition temperature, using internally notched plate specimens tested in tension. The width and thickness of specimens were combined in a single parameter, the ratio of gross width of specimen to thickness of the plate, called the Aspect Ratio (AR). Specimens of equal AR were initially geometrically similar, since notch length and acuity were also held in strict similitude.

The intent of this study was to obtain a separation of geometrical from metallurgical effects in plates from the same heat having variable "as rolled" thicknesses. Since specimens geometrically similar to each other differ only with respect to their absolute scale or size, and since absolute size in itself alone can not affect a dimensionless quantity like transition temperature, differences in behavior of specimens of equal aspect ratio can be attributed only to metallurgical causes, as, for example, relative grain size. A systematic variation in AR in

each of the various plate thicknesses was made, and each of two different steels. Assuming for a given thickness of a given steel, that chemical and metallurgical properties remain constant, any varying effects noted could be attributed to geometry in the form of variable aspect ratio or, in this case, width. By using specimens of different thicknesses, but with equal AR, a determination was made of the effects of metallurgical changes due to rolling.

MATERIALS

The samples used in the aspect ratio program have been given the code designation T-1, T-2, and T-2R. The T-1* steel was furnished in 1/2", 3/4", 1" and 1-1/2" thicknesses, with all plates rolled from the same heat. The T-2 steel was received in 3/4", 1" and 1-1/2" thicknesses, all rolled from the same heat. T-2R designates the 3/4" thick plates obtained by re-rolling a portion of the 1-1/2" thick T-2 steel.

The chemical analysis for these steels is as follows:

Steel Code	C	Mn	P	S	Si
T-1	.16	.93	.013	.034	.02
T-2	.18	.72	.024	.026	.26

T-1 steel is a semi-killed steel of the ABS-B type and the T-2 steel is a silicon-aluminum killed, fine grained steel.

---

*The T-1 steel was given the plate code letter "C" in the report "Further Study of Navy Tear Test" by N. A. Kahn and E. A. Imbembo published in the Welding Journal, February 1950. (9)

The T-2R steel was produced by re-rolling 2 pieces of T-2 steel 1-1/2" thick x 48" wide x 60" long. A reduction to 3/4" thickness was made without cross rolling in 3 passes while maintaining the 48" wide dimension. The 1-1/2" thick plates were in the soaking pit prior to rolling for one hour and fifteen minutes at a temperature of $2240^\circ F$. The finishing temperature was $1650^\circ F$. The surfaces of the re-rolled plates were excellent and relatively free from scale.

The grain size for these steels has been reported to this laboratory by N. A. Kahn* of the New York Naval Shipyard, as follows:

Steel Code	Plate Thickness	McQuaid-Ehn Grain Size
T-1	1/2"	1 to 4
T-1	3/4"	1 to 3
T-1	1"	1 to 3
T-1	1-1/2"	8
T-2R	3/4"	7 to 8

It has been further reported for the T-1 steel that a progressive decrease in the ferrite grain size was observed, with a decrease in plate thickness. The ferrite grain size for the T-2 steel has been reported as 5 to 7 and for the T-2R steel as 6 to 8.

---

*By letter.

The values of yield stress and ultimate stress are given in Table 17.

TEST SPECIMENS AND TEST SCHEDULE

Figure 22 represents the type of specimen used. The dia-meters of the drill holes at the ends of the internal notches are directly proportional to plate thickness, starting with a diameter of 1/32 inch for a plate 1/2 inch thick. The sizes of the drill holes for various thicknesses of plate are indicated in Figure 22.

The aspect ratios tested in the different thicknesses for the various steels are given in the table 18.

Measurement of Elongations and Temperature Control

The elongations of test specimens under load were measured in the direction of tensile loading over a gage length equal to 3/4 the width of any individual specimen. The same clip gage instrumentation as described in Report No. SSC-21[1] was adapted to longer or shorter gage lengths by using an adapter.

Temperature control was obtained as described in Part I of this report.

TEST RESULTS

Data

All data are given in Report No. SSC-44[3] covering this subject. The present report only gives summaries of the basic data, in the form of maximum unit stress, unit energy, and

ASPECT RATIO $= \dfrac{W}{t}$

GAGE LENGTH $\dfrac{3}{4}$ W

DRILL HOLES

$\dfrac{1}{4}$ W

W
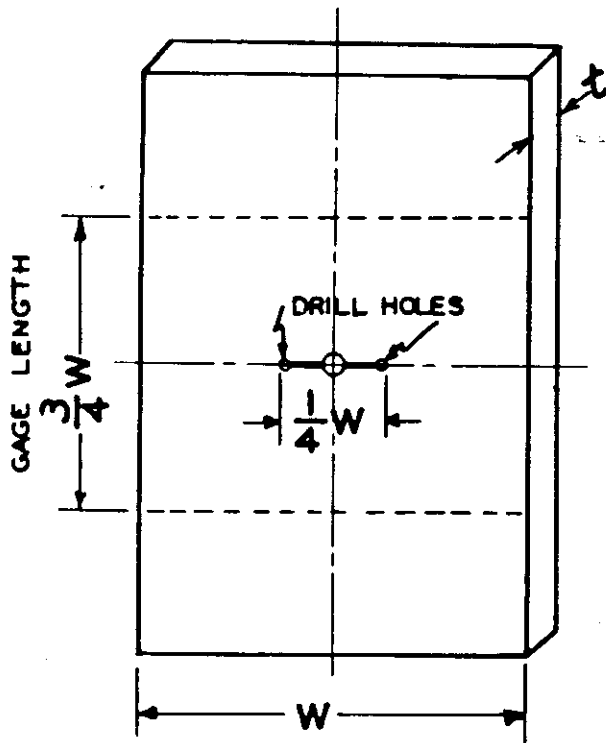
t	DIA. OF DRILL HOLES
$\dfrac{1''}{2}$	$\dfrac{1''}{32}$
$\dfrac{3''}{4}$	$\dfrac{3''}{64}$
$1''$	$\dfrac{1''}{16}$
$1\dfrac{1''}{2}$	$\dfrac{3''}{32}$

DRILL HOLES

SAWCUT

ENLARGED VIEW

$\dfrac{1}{4}$ W
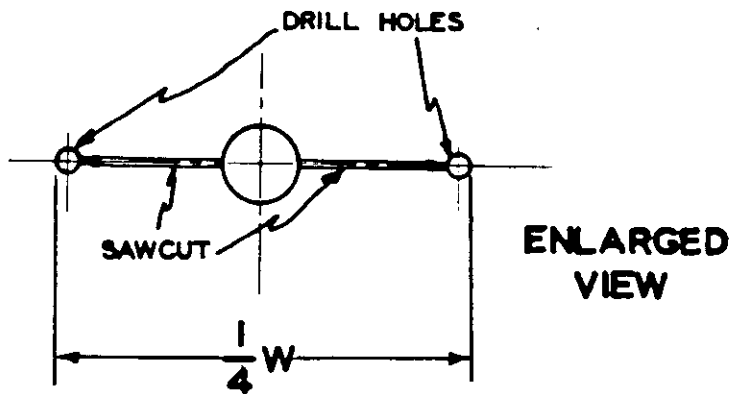
FIG. 22

TYPE OF SPECIMEN

SWARTHMORE COLLEGE

9-6-49

transition temperature, as reduced from data on all the specimens in each group.

Average Maximum Unit Stress

Unit stress at maximum load is summarized in Tables 19 and 20; it is determined by dividing the maximum load by the net cross-sectional area of the specimen at the notch. The values given in Tables 19 and 20 are separately given for all specimens exhibiting either a shear failure or a zero shear failure.

Unit Energy

The Energy absorbing capacities of a given steel in different aspect ratios may be compared by considering single values as averaged for all specimens tested under equal conditions. This unit energy is designated by the symbol u. For each of the specimens contributing to the average it is the result obtained by integrating the load-elongation curve to the point of maximum load and dividing by the whole volume of the plate between gage lines, with no allowance for the notch. If W is width and t thickness, this volume is

$$W \times 3/4 \ W \times t$$

Thus u = Energy ÷ $3/4 \ W^2 t$ inch-pounds per cubic inch.

Table 19 summarizes unit energies to maximum load for the various specimens of T-1 steel. These values are given only for specimens failing in 100% shear or zero percent shear, but in each

case the averages were extended to all relevant specimens.
Table 20 summarizes results for T-2 and T-2R steels in a similar
way. Energy absorbed beyond maximum load has not been considered
in the present analysis, though its values are recorded in pre-
vious reports,[1],[2],[3]

DISCUSSION OF TEST RESULTS

Throughout this project the aim has been to avoid any sort
of commitment, especially of an implicit nature, to any specific
set of ideas; to report factual data in full, and thus to leave
the way open for free, possibly for conflicting, interpretations.
Thus, among the plotted data on temperature effects, no curves
have been drawn. Of course the very nature of the test bears an
implication that temperature has a prime influence on the be-
havior of the steel; the tests are intended to provide unprejudiced
data as to the nature of this influence. In following these aims
a standard procedure has been used throughout and it has been
described in detail in the progress reports.

One might hope for data that would speak for themselves in
a convincing way in answer to certain specific questions. Such
a question is this: what is the highest temperature at which cold
brittleness of a given sample of steel might impair its usefulness
in ship hull construction? But to this question neither these
nor any other tests give a clear-cut answer. Any one may view
these data against his own background of experience and judgment
in reaching his own conclusions.

This does not mean that we have had no idea as to what conclusions might withstand critique and finally be found valid. Rather we have had two different ideas. Instead of presenting simply the conclusion on which we finally agree, or framing conclusions so vaguely as to make them useless for further thought on this subject, we prefer to describe the course of our own thought as it developed during work on the project.

The guiding thought in choice of this type of specimen, now as ten years ago, is that it is a compromise between two extremes. On one hand, specimens so small and in form so different from full scale structure as to bear to it no resemblance at all are widely used. The validity of results of tests with such specimens depends on the idea that features of the behavior of a sample of metal as demonstrated in such small specimens will persist in a full scale structure made of the metal thus sampled, regardless of geometrical differences, and, particularly, regardless of size.

At the other extreme is the idea that both geometrical form and size affect cold brittleness; strictly, therefore, only the full scale structure can speak for itself, and the only source of information lies in the study of service casualties.

The compromise offered by the wide plate specimens is based on the idea that the effects of geometrical form and of size can be ascertained. It is a laboratory specimen which reduces differences from full-scale structure in form and size to the point where the allowance which must be made for these differences can be reduced to a moderate amount.

With respect to form, the specimen differs from the full-scale deck plating of a ship mainly in two particulars: (a) in use of a standarized notch, and (b) in width. Standardization of the notch is necessary in order to obtain systematic data. The actual spread in severity of service notching, the relative severity of the standard notch, and the influence of notch severity on behavior -- all these are subjects lying outside the limits of the purpose of these tests.

The Role of Similitude

With respect to size, the wide plate specimen is equal to full-scale deck plating in thickness. A primary object of the project is to study the effect of width on cold-brittleness under the condition of constant thickness as rolled. Ships' decks, however, are not all 3/4 inch thick.

In study of cold brittleness in different thicknesses, each different thickness could be regarded as a different case, unrelated to other thicknesses. Since rolling down to reduced thickness alters the metallurgical nature of a sample of steel, there is ground for regarding plates of different thickness as being quite simply different sample of steel. Our data permit any one who so wishes to follow such an interpretation.

But it ought to be possible to do better than that. A progressive change in thickness produces like progressive changes in all medium steels; rolling down to reduced thickness favors

ductility. But when we proceed to evaluate this effect we must
answer this question: How are samples of different thickness
to be compared with each other? Are the specimens to be of equal
width, or should all the conditions of full geometricl similtude
be applied?

It is possible that this question could be by-passed for
the wide-plate specimens by simply evaluating width-effect separ-
ately for each thickness. But if any broad conclusions about
the systematic influence of thickness on behavior are to be
drawn, this question cannot be evaded. Thus between the wide
plates and small test specimens the obvious and primary differences
are those of form and size. Before the results of tests with
small specimens can be translated into terms of wide plates,
and thence to full-scale structure, the effect of these differences
must be understood. Otherwise the use of such specimens implies
that they give information as to the inherent qualities of the
steel, which is equivalent to the assertion that the differences
in form and size are without any effect on the essential behavior
of the metal. No one can assert that this has been proved, and
we do not believe that it is true.

Aside from this practical need for a better understanding
of the role of similitude, it has a more general interest. Re-
peated attempts have been made to determine whether data from
specimens in strict similitude, and differing only in scale-factor,

actually conform to the laws of similitude, without "size-effect", that is without effects which can be attributed to differences in size alone. A series of eleven tests of this nature have been described by Earl Parker[10]; special effort was made to obtain identity of material and the initial dimensions were in strict geometrical similitude, yet at equal temperatures the thicker specimens were less ductile. The author explains this by the presence of an incipient crack at an early stage in deformation. More extensive tests are reported from the University of North Carolina[11] ending with the conclusion the "size effects in plastic flow are small. Prominent effects are associated with the initiation and propagation of cracks."

An extensive review of this matter, with special reference to the notched bar impact test, was made by Fettweis in 1929[12]. He points out that F. Kick, in 1885, stated the Law of Similitude for plastic deformation as follows: "If two geometrically similar bodies of identical material (gleicher Beschaffenheit) are deformed by external forces similarly applied in such a way that the geometrical similitude continues to be maintained, then energy absorbed is in the ratio of the volumes of metal and forces are in the ratio of the areas.

"When these conditions are satisfied, the ratios are as stated, not only for the body as a whole, but also for its infinitesimal parts. The corresponding stresses in the two bodies are thus equal."

Although in numerous notched bar tests by many investiga-
tors the equality of the ratios mentioned by Kick is not main-
tained when scale factor is varied, yet this can be ascribed
to failure to satisfy the necessary conditions. It can hardly
be doubted that if the conditions could be met the requirements
of similitude would be satisfied.

In the present static tests deviations from behavior in accord
with similitude occur mainly with respect to two particulars:
(a) metallurgical constitution of the material, and (b) mainten-
ance of similitude in the details of the strain patterns. Tem-
perature, being without geometrical dimensions, would have no
geometrical influence and actual temperature effects would have
to be attributed to inherent qualities in the metal. So far as
similitude is concerned, samples of the same metal at different
temperatures are, in effect, of different metals.

If the two deviations from similitude as mentioned could
be controlled, it would be necessary only to duplicate, on a
reduced scale and in identical material, a segment of full-
scale structure, load it correctly in the laboratory, and from
the results infer what plastic behavior might be expected of the
full-scale prototype.

In planning the present tests we were also concerned with
these more distant considerations. But in any case, whatever use
of the data might later be made, it was clear that the different

-38-

widths for each thickness should be chosen so as to give homo-
logous series of values of the dimensionless ratio of width
to thickness, the "aspect ratio".

Nominal Stress at Maximum Load

The unit stress values from Table 19, as averaged for all
specimens failing in 100% shear, are plotted on aspect ratio
in Figure 23. The plot shows that strength in each thickness
gradually but consistently decreases with increasing aspect
ratio. This gradual reduction can only be due to increased
width since both acuity and metallurgy are constant for any
given thickness.

Considered with reference to then ultimate tensile strength
in an un-notched specimen (UTS) as given in Table 17, these data
indicate a complex situation. It has long been accepted that
UTS in an un-notched bar is not much affected by width but the
presence of the notch has the strange effect of introducing a
regular decrease in strength with increasing width at constant
thickness. One might expect that adding metal at a distance
from the notch would diminish the overall influence of the notch,
but the actual effect has a contrary sense. It is the narrower
specimens, in which the average distance of metal from the notch
in the net section is less, that are the stronger. Indeed, in
both 1/2 and 3/4 inch thicknesses, in the narrowest specimens,
notching actually raises the tensile strength above the un-notched
value.

Comparing the different thicknesses of T-1 steel (in 3 of the 4 cases) at any given aspect ratio, strength of the notched specimens runs parallel to that of the un-notched bars. The 1-inch bar in Table 17 shows an anomaly not seen in the notched specimens. Aside from this anomaly, the curves in Figure 23 for the different thicknesses would be nearly superposed if strength were plotted as a fraction of UTS.

At one stage in the analysis of these data it was thought possible to sift out evidence that might indicate a deviation from the conditions of strict similitude such that two specimens, differing only in scale factor, might yet not be equal to each other in strength. Except for the anomaly of the 1-inch bar, no such deviation appears. But it happened, in the search for geometrical effects, that strength was plotted on gross width, regardless of thickness, instead of on aspect ratio. The result, as seen in Figure 24, is that the curves for the four thicknesses are nearly superposed. A hasty conclusion was suggested, that strength might be affected only by width and not at all by thickness. The loss of strength as width increases is well marked, but at any one width all thicknesses have nearly the same strengtn.

Further study reveals, however, that this is a case of mutual cancellation of two opposite effects which happen to be nearly equal. When plates geometrically similar are compared (as at equal aspect ratios in Figure 23) the thicker plate has a lower
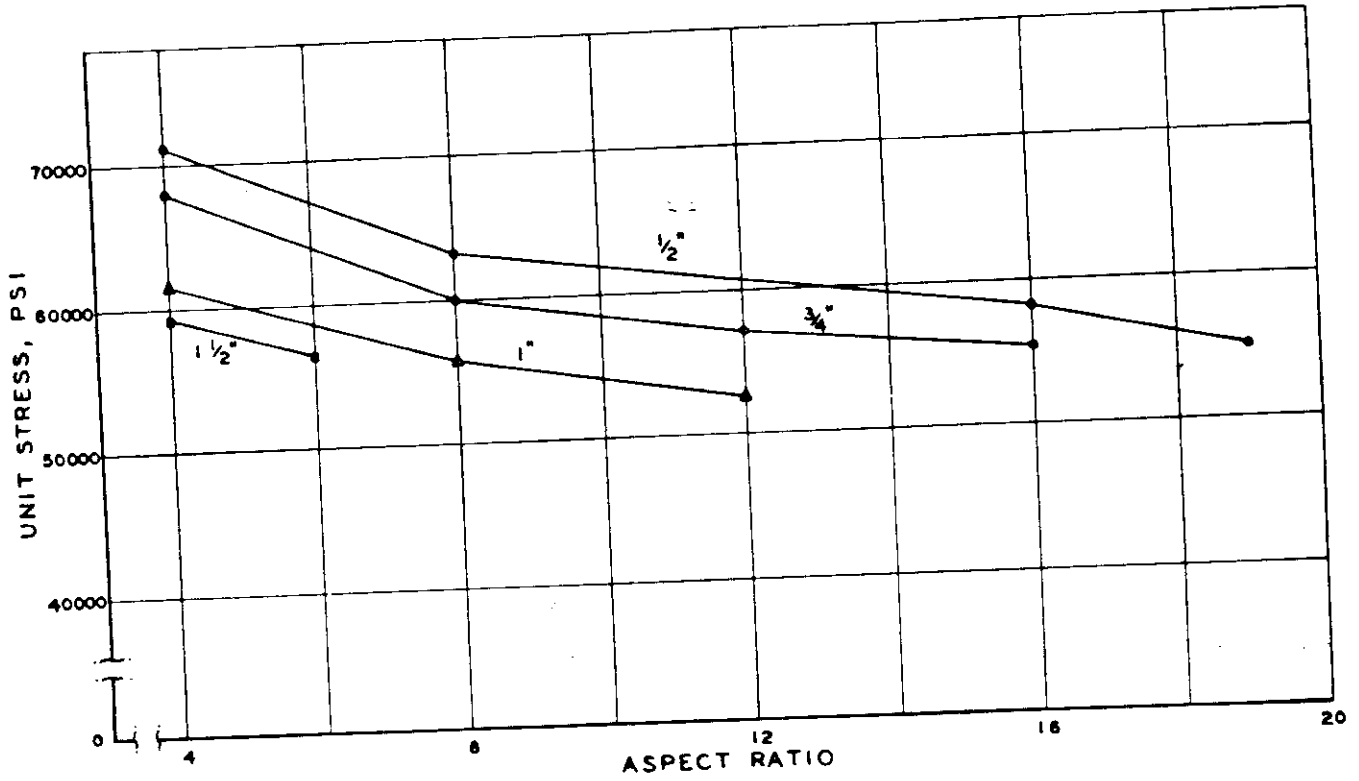
FIG. 23   VARIATION IN UNIT STRESS AT MAXIMUM LOAD
FOR VARIABLE THICKNESS AND ASPECT RATIO,
T-1 STEEL, 100% SHEAR FAILURES.

SWARTHMORE COLLEGE
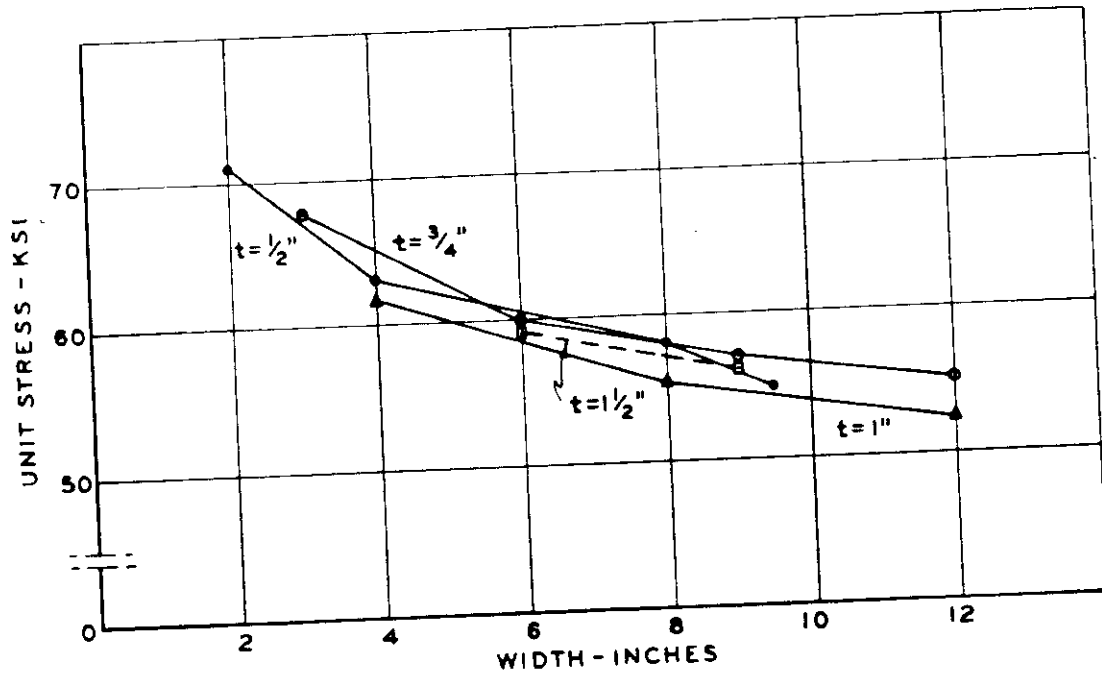
FIG. 24   VARIATION IN UNIT STRESS AT MAXIMUM LOAD
FOR VARYING WIDTH AND THICKNESS, T-1 STEEL,
100% SHEAR FAILURES

SWARTHMORE COLLEGE

strength; it is, however, wider as well as thicker. If its width is cut down to match that of the thinner plate, its strength is increased. These opposite effects come near to cancelling each other when aspect ratio is multiplied by thickness and comparison is made, as in Figure 24, at equal width.

The differences between thicknesses at equal aspect ratios in Figure 23 are metallurgical differences. No reason is seen for doubting that if these metallurgical differences could be eliminated, notched specimens of all scale-factor values, but at the same aspect ratio, would have the same nominal strength at maximum load.

Unit Energy Absorption

In Figure 25 the unit energy to maximum load for specimens failing in 100% shear is plotted against aspect ratio for plates of T-1 steel. For equal aspect ratios the 1/2 inch thick plate absorbs more energy per cubic inch than the thicker plates though the differences due to thickness are less in the higher aspect ratios. In all thicknesses without exception the energy value rises as aspect ratio diminishes, and this rise is sharpest at the smallest values of aspect ratio.

Unit energy for specimens failing in zero percent shear shows the same trend with diminishing aspect ratio as specimens failing in 100% shear, and the same effects of thickness, as is seen in Table 19. The values of unit energy are lower for zero percent

shear failures than for 100% shear failures at aspect ratios of 8 and greater, but at aspect ratio 4 the two values are equal within the limits of precision of the tests. Additional energy data are given in Table 20 for T-2 and T-2R steels. They follow the same trends noted for T-1 steel but the energy values at equal thickness and aspect ratio values are smaller than in T-1 steel.

At the moment when Figure 24 seemed to show that strength depended on width only, data on unit energy were also plotted on width as in Figure 26. The result, however, is now different from that in Figure 24 in that the curves for different thicknesses, as plotted on width, are displaced so far from their positions in Figure 25 as to reverse their order and make it appear that the thicker plates have the greater capacity for absorbing energy. In order to bring the curves together, the necessary adjustment of the abscissa is less drastic than before, and instead of multiplying aspect ratio by the thickness it is found to be enough to multiply it by the square root of the thickness, as in Figure 27.

We conclude that the metallurgical gain with respect to energy absorption in thinner plates is more than offset by the loss incurred in comparing them with thicker plates at equal widths rather than by giving the thinner plate a smaller width by equating aspect ratios.
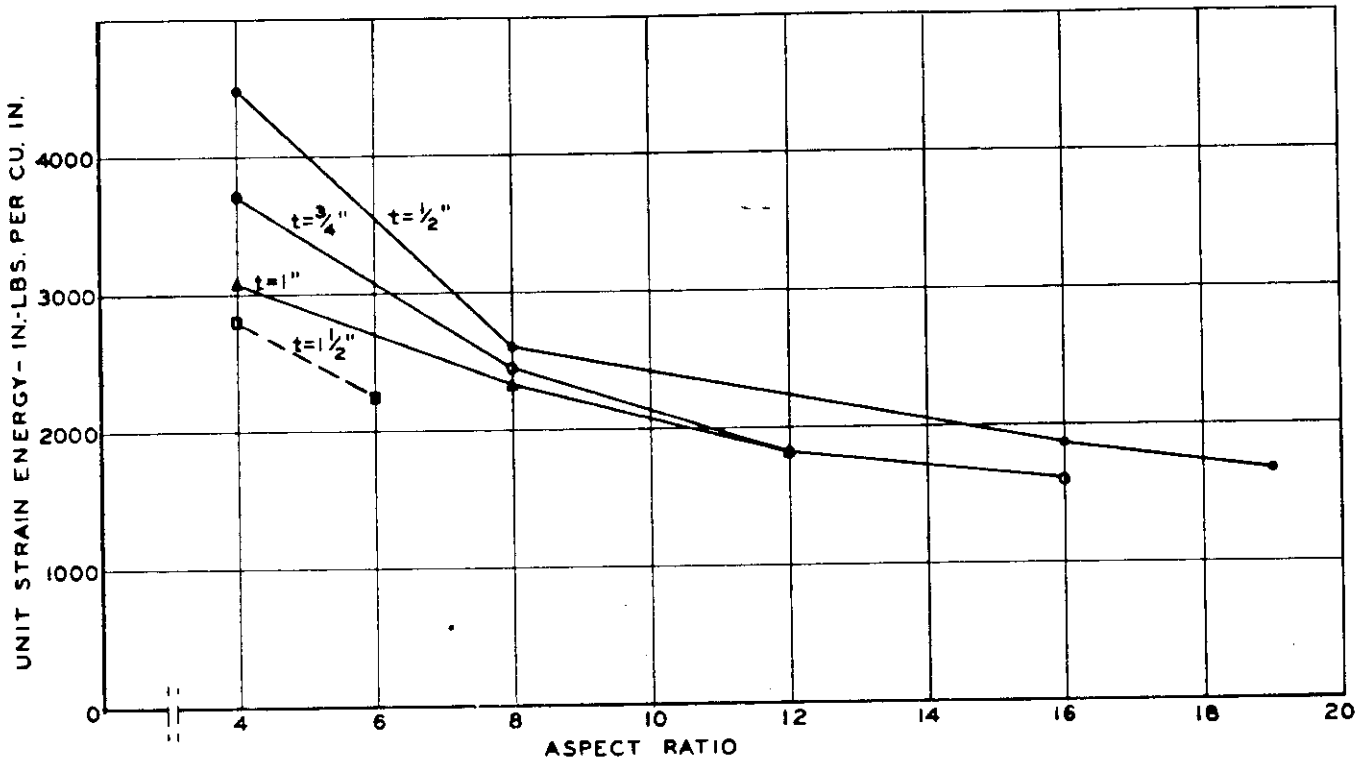
FIG. 25   AVERAGE UNIT STRAIN ENERGY TO MAXIMUM LOAD FOR VARYING ASPECT RATIO AND THICKNESS, T-1 STEEL, 100% SHEAR FAILURES
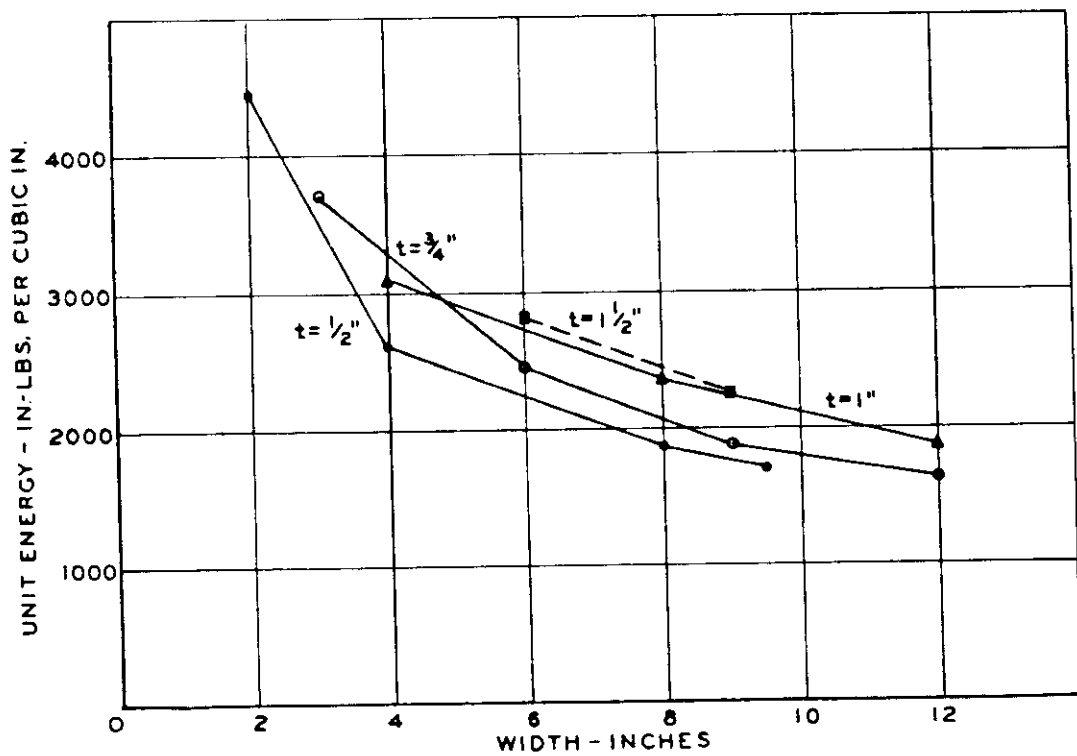
FIG. 26   AVERAGE UNIT STRAIN ENERGY TO MAXIMUM LOAD FOR VARYING WIDTH AND THICKNESS, T-1 STEEL, 100% SHEAR FAILURES
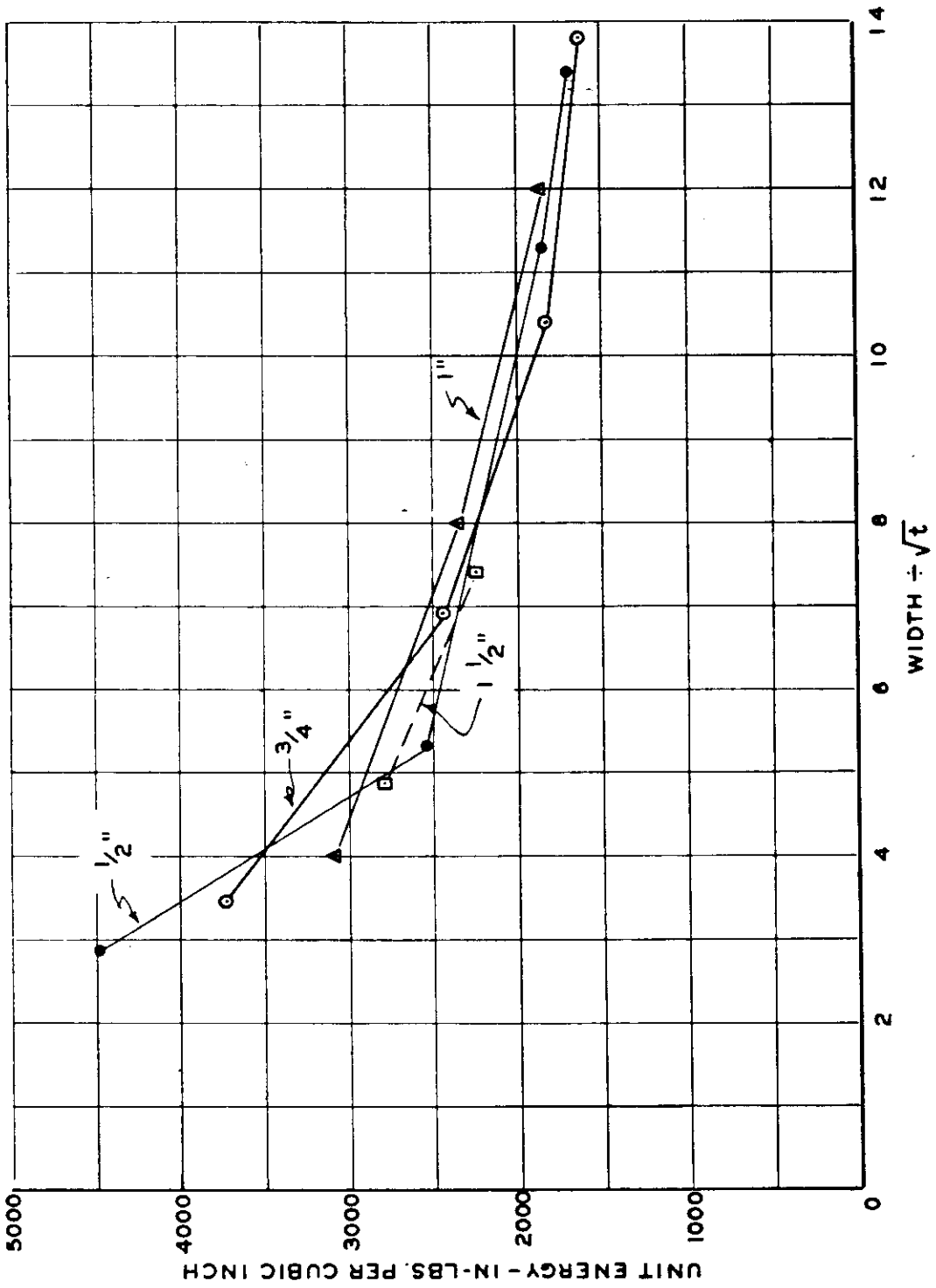
FIG. 27   AVERAGE UNIT STRAIN ENERGY TO MAX. LOAD,
PLOTTED AGAINST WIDTH $\div \sqrt{t}$,
STEEL T-1, 100% SHEAR FAILURES

SWARTHMORE COLLEGE

In Figure 26 as in Figure 24, the inequality of unit energy values at equal aspect ratios is again seen to be reducible by an adjustment of the scale of abscissae as in Figure 24. But comparison of Figure 23 with Table 17 shows that when allowance is made for the differences in strength as measured in un-notched bars, the curves for different thicknesses are superposed about as well as by shifting the scale of abscissae. In Figure 25 the metallurgical differences in ductility would serve equally well to explain the inequalities without resorting to the device used in Figure 27.

As for a numerical check form the actual data, it is regretted that no data on ductility in the un-notched bars were available. It is well known, however, that reduction in area becomes smaller as thickness increases; since such measurements are subject to scatter it is as much as could perhaps in any case be said if we note that energies in equal aspect ratios in the notched specimens are affected in a like way as thickness increases.

In addition to simple differences in ductility, as measured by reduction in area, there is also the other respect in which the conditions of similitude may not be completely satisfied, namely, that of similitude in strain patterns. The stage of deformation at which comparisons are made in Figure 25 is that of maximum load. On the interesting question as to strain patterns at this stage, in two specimens differing only in scale

factor, we have no direct information. Such data might be taken by making photographic records at a series of stages and on different scales, of grids ruled on the specimens. Such a project was considered but its difficulty and cost barred it from the program of work.

This point is worth emphasis by restatement. The conditions of geometrical similitude in the present tests refer only to the initial state of the specimens before plastic flow has altered their configurations, whereas the energy values refer to a stage of deformation (that of maximum load) in which large local strains have occurred, even to the point of fracture near the apex of the notch. These geometrical changes due to plastic flow are beyond control and the question as to whether or not they follow the laws of similitude is one of fact which could be answered only by observations more detailed than those that were made during the tests. Close study of surface grids on different scales after deformation might have served to determine whether the pattern of deformation in the large specimens could be derived from that in the small ones by a transformation like that of photographic enlargement, as would be the case if similitude continued to be effective throughout the successive stages of deformation, but this work lay beyond the scope of the actual project.

For inferences about similitude in deformation patterns we must therefore rely on indirect evidence. Some such evidence

drawn from work of other investigators has been reviewed in
Reference 13. A study of the details of load-elongation curves
is now being undertaken for the wide plates, somewhat as has
been done by Richard Raring for notched bars in slow bending.[14]
Even the presence of an incipient crack may not greatly disturb
the overall strain pattern, and on this matter observed elonga-
tions may throw some light.

Thus if, as there is some reason to believe, a stage exists
at which the crack, though partly developed, has nevertheless
not yet advanced far enough to affect the broad outline of the
strain pattern, then even at this stage the conditions of simili-
tude may be nearly satisfied. The main question will refer
to the stage at which the deviations from similitude become too
great to be ignored, and particularly how far before maximum
load this may occur.

We again note that, even in different steels, if stress
patterns at a given stage of deformation share in the condition
of similitude, loads are necessarily in the ratio of the squares
of the scale factor. If strain patterns at a given stage of de-
formation share in the condition of similitude, overall elonga-
tions at that stage are necessarily in the ratio of the first
powers of the scale factor. Gross energies, therefore, must be
in the ratio of the cubes of the scale factor. Temperature,
being itself without geometrical dimensions, has no effect pre-
dictable by reference to scale factor.

Transition Temperature

Evaluations were made as described in Part I on diagrams like
Figure 28 of which, however, only the lowest part, relating to
appearance of fracture surface, was found to be needed. Figure
28 is typical of the test results of the entire program except
that in the narrow specimens the energy to maximum load is not
significantly different as between 100% shear and full cleavage
fractures, whereas in greater widths a shift like that which ap-
pears in Figure 28 in total energy may also be seen in energy to
maximum load, and at approximately the same temperature. This
fact is important, and will bear repetition.

In the higher aspect ratios used in the present tests a loss
of capacity for absorbing energy occurs at about the same tempera-
ture range as that in which the appearance of fracture shifts
from 100% shear to zero percent shear. Energy beyond maximum
load drops off to zero, as in Figure 28; energy up to maximum
load shows a partial reduction; the total energy (as measured in
an impact test) is a simple summation of these two contributions.
If there is a difference between the temperature of energy transi-
tion and that of fracture transition in this case, it is not great
enough to be revealed by the experimental method used.

With respect to the energy to maximum load, Figure 28 is
typical of narrow specimens. At the temperature at which the
shift occurs in appearance of fracture and in energy beyond
maximum load, no similar shift occurs in the energy up to maximum

FIG. 28

SUMMARY FOR ALL BLOCKS

1/2" THICKNESS ASPECT RATIO 4

STEEL T-1

SWARTHMORE COLLEGE
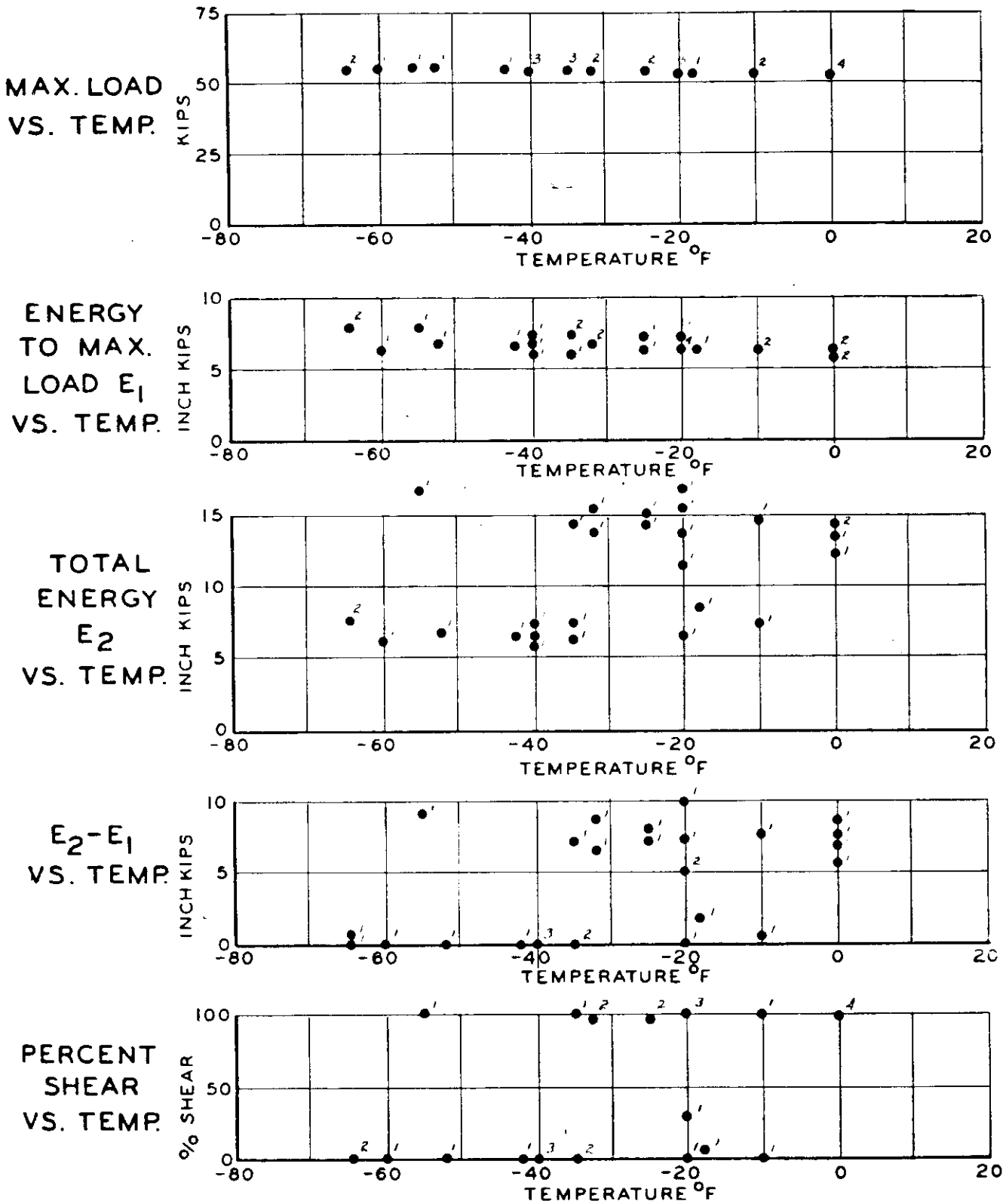
NOTE:

NUMBER ADJACENT TO
PLOTTED POINT INDICATES
NUMBER OF SPECIMENS.

load. It is possible that tests at lower temperatures a loss
of energy to maximum load would occur. All that can be concluded
from the present data is that in the narrow specimens no loss
of energy to maximum load occurs in the temperature range in
which fracture shifts from 100% shear to zero percent shear
and energy beyond maximum load drops to zero.

Transition temperatures based on appearance of fracture
are given in Table 21 for T-1 steel and in Table 22 for T-2
and T-2R steels. These temperatures are given both as ranges
and as single values, as described in Part I.

Figure 29 is a plot of the single values of the temperature
of transition against aspect ratio, for T-1 steel in four thick-
nesses. At any given aspect ratio, transition temperature is
higher in thicker plates, with a single exception. For a given
thickness of plate, the effect of aspect ratio on transition
temperature shows a clearly marked trend toward higher values
as aspect ratio rises.

Figures 30 is a repetition of Figure 29 with a second para-
meter added, width of the specimen. In order to complete this
diagram, an extrapolation of the test results in 3/2 inch thick-
ness was made to widths of 4 and of 10 inches. Figure 30 shows
that thicker plates have notably higher transition temperatures
than thinner plates, regardless of whether aspect ratio or width
is considered to be constant.
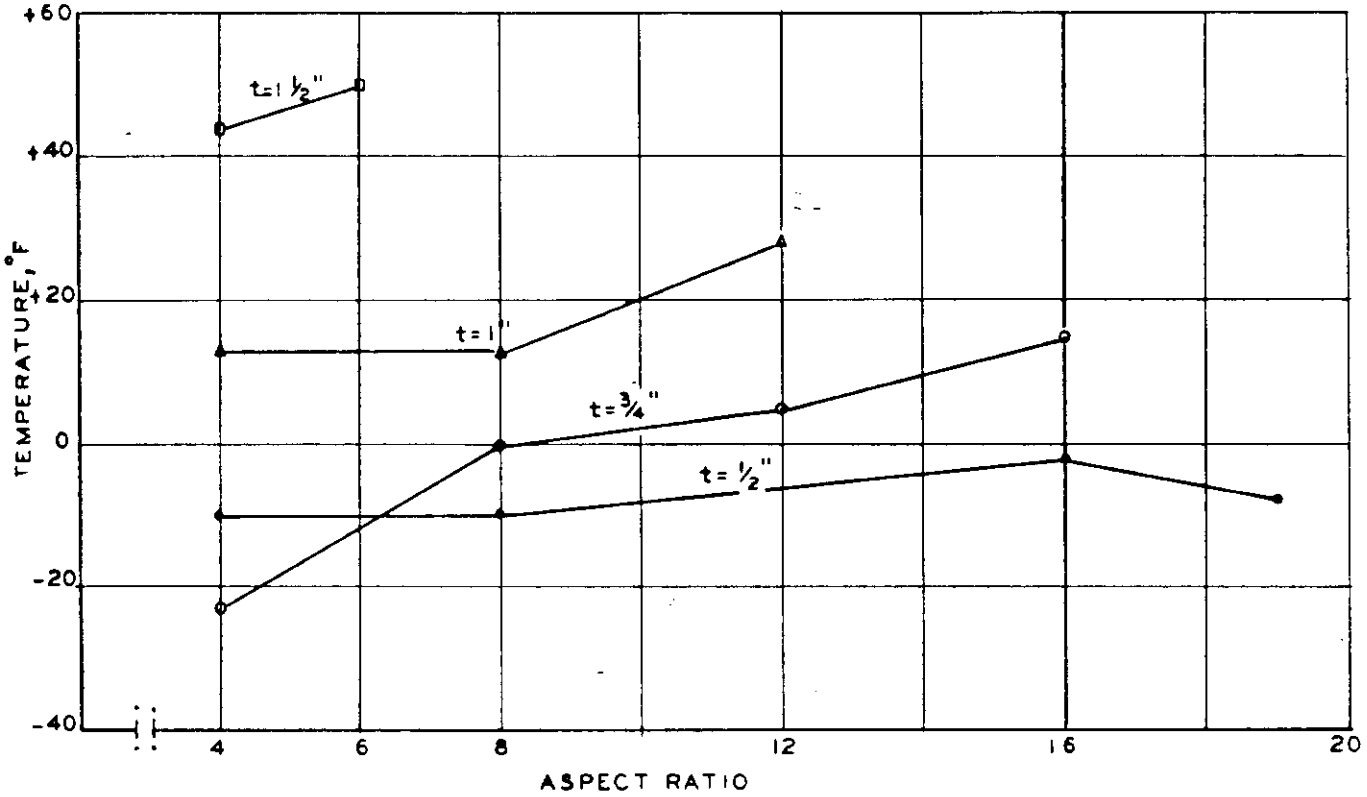
FIG. 29   TRANSITION TEMPERATURE FOR T-I STEEL
WITH VARYING ASPECT RATIO & THICKNESS
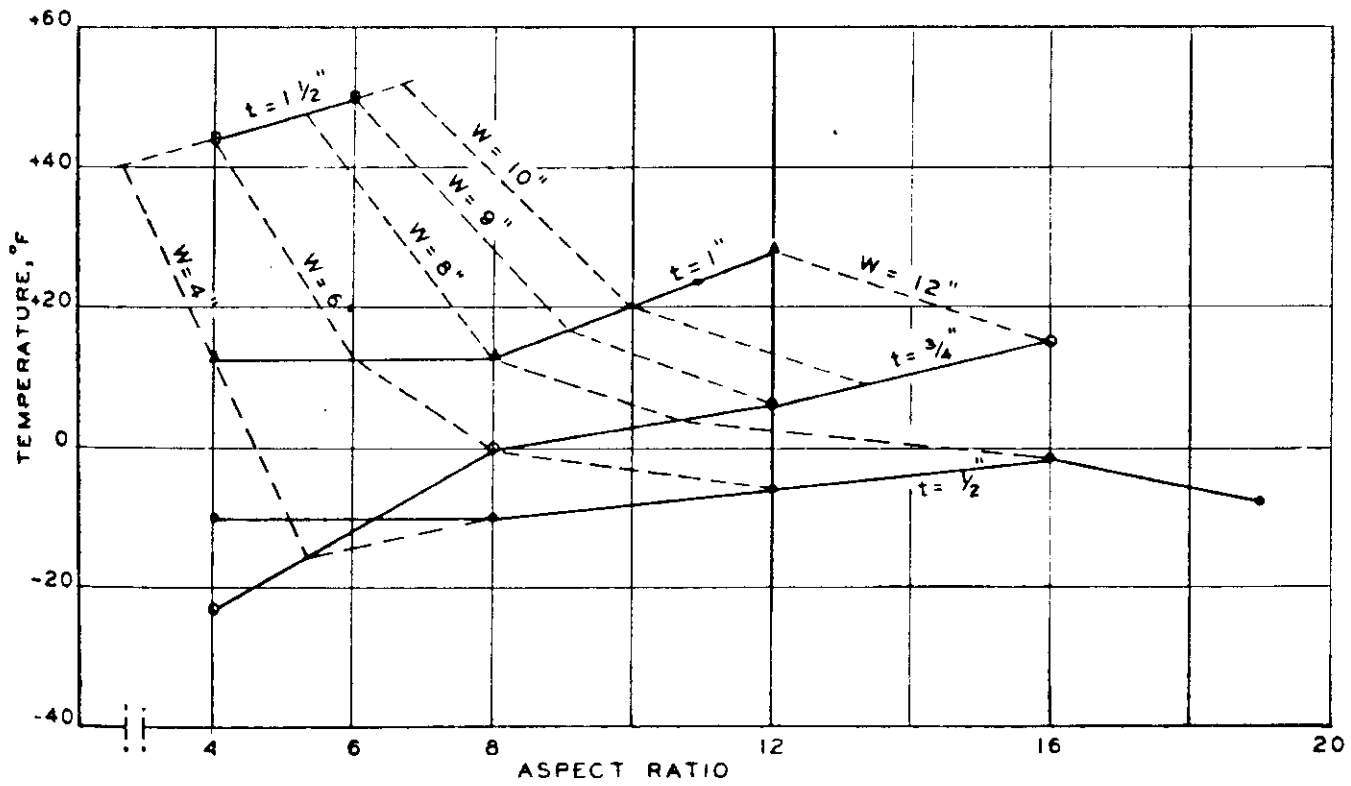
FIG. 30   TRANSITION TEMPERATURES FOR T-I STEEL, SHOWING
EFFECT OF ASPECT RATIO, THICKNESS AND WIDTH OF
SPECIMEN.

The question now arises: what part of this increase in transition temperature with thickness may be due to geometrical differences and what part to metallurgical differences?

The effects of geometrical differences can be identified directly in the absence of metallurgical differences, and we have data of this kind in the variations with width at constant thickness. The fact of a moderate rise in transition temperature with width, though somewhat obscured in Figure 29, is recognizable and in accord with other data. But this leaves the question as to the effect of thickness still open.

Conversely, the effects of metallurgical differences could be directly determined only in the absence of geometrical effects; this condition will be realized in equality of aspect ratios if, in fact, there is no "size effect".

It was at one moment suspected that dimensional similitude might not completely eliminate geometrical effects, and the question was raised whether isolation of metallurgical effects might not require comparison of the various thicknesses on some basis other than equality of aspect ratios. The fact is that the rise in transition temperature with thickness is so great that no replotting on variables other than aspect ratio could obscure it, and no width effect can offset it. From this we conclude that the effect of thickness on transition temperature is mainly or wholly metallurgical, and to assume it to be wholly so is a close approximation to the truth. While the proof stops just short of being complete because of uncertainty about strain

patterns, we may be sure that the present data contain no evidence adverse to this conclusion.

Summary

The facts about offsetting or compensating effects of metallurgical and of geometrical conditions, as they appear in the present data, may be summarized as follows:

(a) Figures 23 and 24 show that metallurgical increase in notch tensile strength due to a reduction from 3/2 to 1/2 inch thickness is about the same as the loss of strength due to the higher aspect ratio in thinner specimens of equal width.

(b) Figures 25 and 26 show that metallurgical increase in unit energy to maximum load due to rolling down from 3/2 to 1/2 inch thickness is smaller than the loss due to the higher aspect ratio in thinner specimens of equal width.

(c) Figure 27 shows that in order to compensate for metallurgical increase in energy value in thinner specimens, width must be reduced only in the ratio of the square root of thickness rather than in the ratio of the first power of thickness.

(d) Figures 29 and 30 show that the metallurgical reduction in transition temperature due to rolling down from 3/2 to 1/2 inch thickness is greater than the loss in such improvement due to the higher aspect ratio in thinner specimens of equal width.

(e) The decrease in transition temperature noted in (d) is too great to be offset by any geometrical effect of thickness.

No change in scale on the width axis would serve to superpose the curves in Figure 29 for the various thicknesses.

(f) Of the three variables, strength, energy, and transition temperature, no two show the same relation between offsetting metallurgical and geometrical effects. No single systematic adjustment of geometrical conditions can harmonize the observed disparities.

CONCLUSIONS - PART II

It is concluded that:

(1) Figures 23, 25, and 29, in which the three variables are plotted against the dimensionless ratio of width to thickness, represent the procedure best adapted to analysis of these data.

(2) Transition temperature remains unaffected by changes in scale factor so long as similitude extends to the deformation patterns and if metallurgical differences are excluded.

(3) In similar specimens transition temperature is higher as specimen size increases. Since the geometrical differences between the specimens are completely described by the difference in scale factor, the observed differences are an effect of the metallurgical changes due to rolling.

(4) However, in plates of equal thickness (and hence equal metallurgically) transition temperature rises with width.

(5) We prefer to state conclusions (3) and (4) in more general terms by saying that when aspect ratio is constant, transition temperature is affected only by metallurgical differences, but regardless of thickness, transition temperature rises with aspect ratio.

PART III

by

S. T. Carpenter

A STUDY OF PLASTIC DEFORMATION BY STRAIN ENERGY DISTRIBUTION*

INTRODUCTION

Part III is a digest of a former Progress Report[4] which presented the results of an exploratory study to determine the energy distribution in notched steel plates stressed in tension. This study placed its emphasis on obtaining a better insight of the distribution of plastic flow through the means of energy absorption as affected by both geometry and temperature.

The plan of investigation was based upon the determination of unit-strain energy absorption and its distribution. Whereas it is generally impracticable to calculate stresses in the plastic strain range, it is possible to calculate strain energy. The octahedral theory was used in computing unit strain energy where strain values were received from displacement measurement made on a surface grid.

SPECIMENS AND PROCEDURES

Specimens

Three 12" wide x 3/4" thick x 24" long steel plates of fully-killed "W" steel were used. Figure 31 shows the internally-notched tensile specimen. The notch is 3" wide and terminates in two holes

---

*Summarized from investigations of S. I. Liu and S. T. Carpenter, See reference (4).
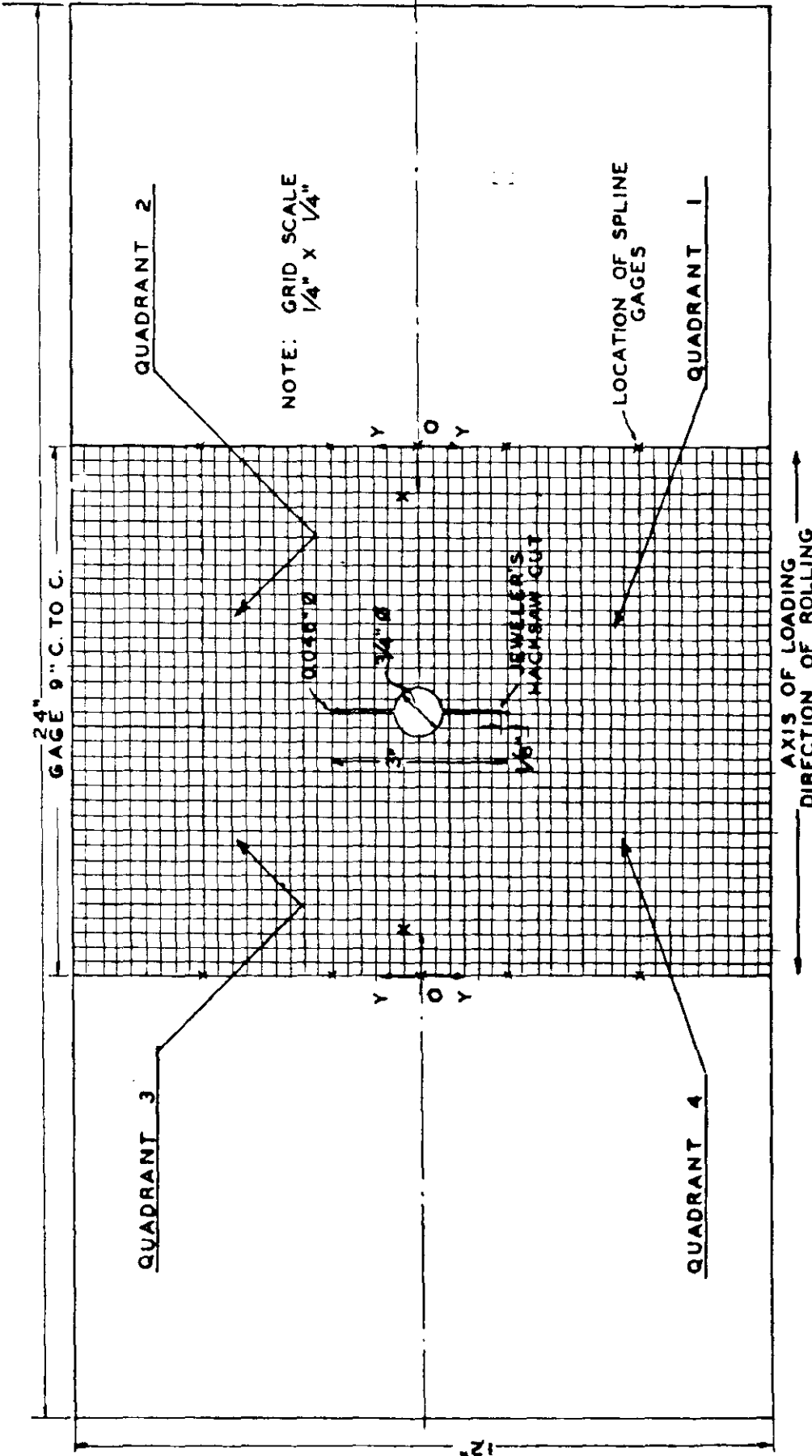
FIG. 31   TEST SPECIMEN FOR STRAIN ENERGY DISTRIBUTION

SWARTHMORE COLLEGE
12-29-49

of 0.046" diameter. The basic grid lines were 1/4" apart, while 1/16" grid lines were used in one specimen to be noted later. The grid layout was on only one surface of the plate and covered the area between the gage lines which were 9" apart. The 24" long specimens were welded to thick and headers.

The three specimens used, with testing and loading schedules, were as follows:

Specimen W-29-4: Tested at 70°F. Grid measurements made after the loads producing an observable crack at 0.046" dia. hole (277,000 lbs), 295,000 lbs., 325,000 lbs. and at a maximum load of 352,700 lbs. Approximately one week intervals between loadings after initial load.

Specimen W-29-3: Tested at 10°F. Grid measurements made after loads producting an observable crack at 0.046" dia. hole (277,740 lbs.), 295,000 lbs. and at the fracture load of 325,000 lbs. Approximately one week intervals between loadings after initial load.

Specimen W-29-14: Tested continuously to fracture at a temperature of 70°F, and grid measured. (1/6" grid layout in central transverse strip 3" wide).

Physical data to determine the octahedral stress-octahedral strain function were obtained from bars of "W" steel having a diameter of 0.650".

Procedures

Temperature control and strain gaging procedures on the 9" gage length were the same as outlined in Part I of this report.

The deformations or displacements of the grid were measured in a milling machine accurate to 0.001". Grid measurements were

made before testing to provide a reference system. The point
"O" shown on Figure 31 was the origin of a Cartesian system of
coordinates, where the x, y, and z directions coincide with the
longitudinal transverse, and thickness dimensions of the plate.
Test specimens were removed from the testing machine after each
loading and approximately a week elapsed between unloading and
reloading to allow for grid measurements.

RESULTS AND DISCUSSION

Strain Energy Distribution

Figures 32 and 33 show the unit strain energy distribution
at maximum load for one quadrant of specimen W-29-3 tested at 10^OF
and specimen W-29-4 tested at 70^OF. The values given for each
quadrant are the average of values found for all four quadrants.
Figure 34 shows the distribution in all four quadrants at frac-
ture for specimen W-9-14 tested continuously at 70^OF. The dis-
tribution of strain energy is shown by means of contours passing
through points having equal values of unit strain energy. The
earlier report[4] also presented the strain energy distribution
diagrams for intermediate loads as given in the loading schedule.

Figures 32 and 33 indicate that the primary direction of
propagation of plastic deformation up to maximum load is gen-
erally in the direction of diagonals extending from the end of
the notch to the edge of the plate. A comparison of Figure 33
with Figure 34 illustrates that the primary direction of propa-
gation of plastic deformation after maximum load follows the
direction of the fracture line.
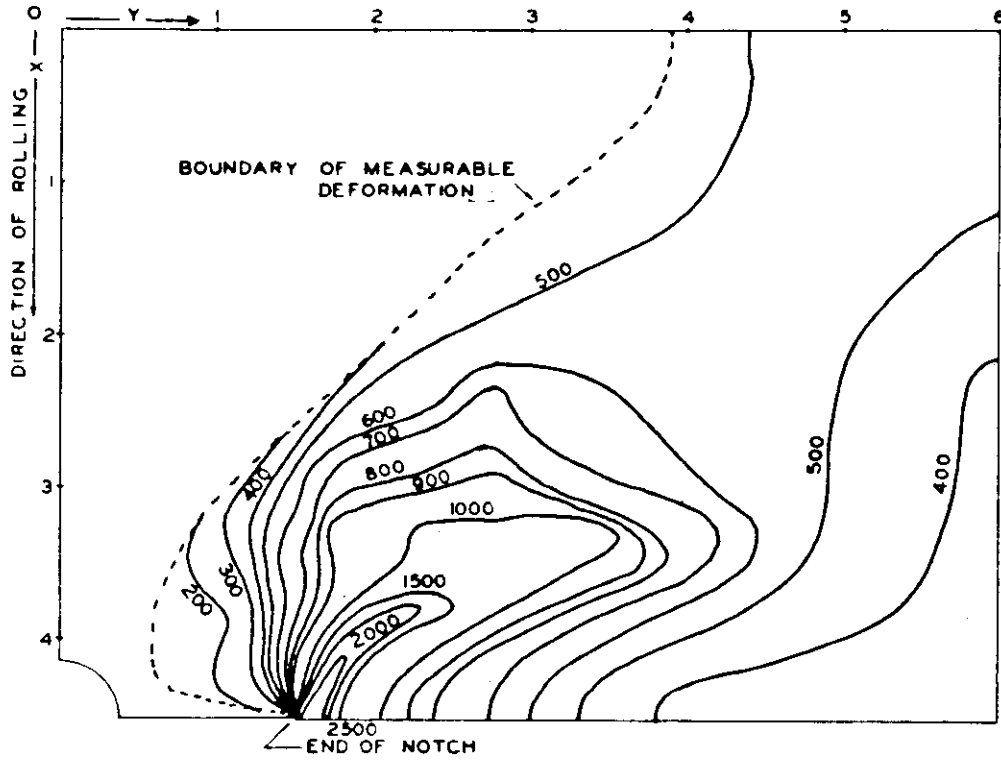
FIG. 32 UNIT STRAIN ENERGY DISTRIBUTION ON THE SURFACE OF A 12" X 3/4" NOTCHED SPECIMEN, W-29-3, LOADED TO 325,000 LBS. (FRACTURE) AT 10° F.
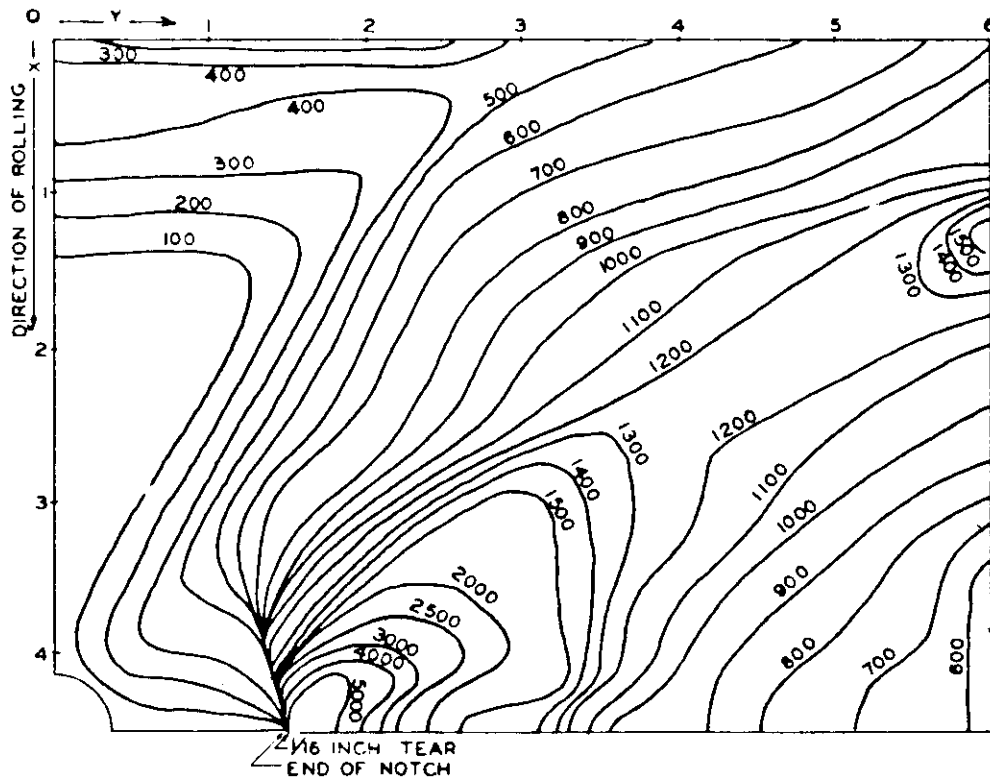
FIG. 33 UNIT STRAIN ENERGY DISTRIBUTION ON THE SURFACE OF A 12" X3/4" NOTCHED SPECIMEN, W-29-4, LOADED TO 352,700 LBS. MAX. LOAD AT 70° F.
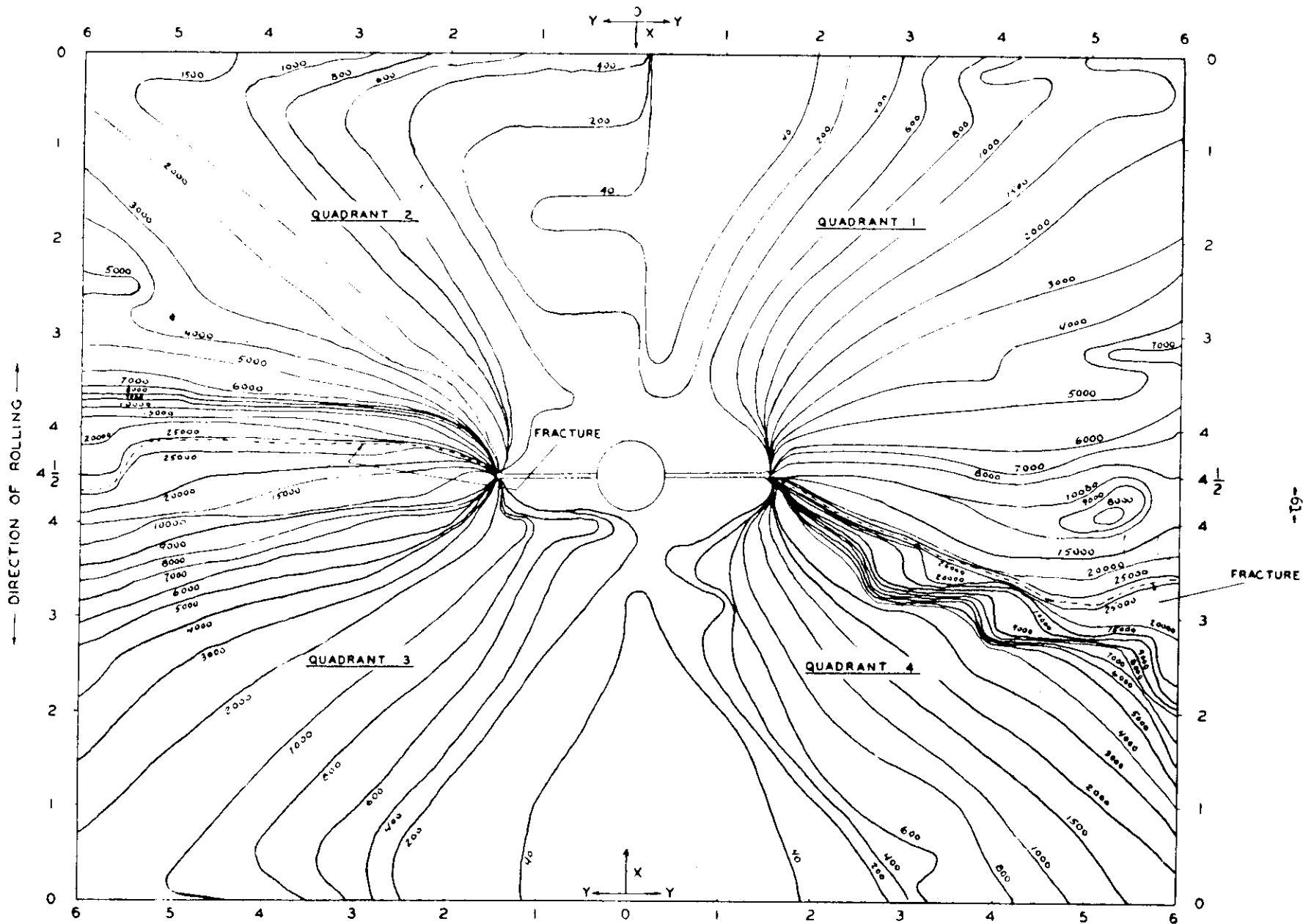
FIG. 34   UNIT STRAIN ENERGY DISTRIBUTION ON THE SURFACE OF A 12"X $\frac{3}{4}$" NOTCHED SPECIMEN, W-29-14, TESTED
TO FRACTURE AT 70°F.   (X,Y IN INCHES)

SWARTHMORE COLLEGE
6 - 15 - 50

The unit energy values in the immediate zone in the
notch and at the fringes of the fracture line for specimen W-29-14
could not be obtained. To do this with precision would require
a more accurate grid measuring system and a finer grid. The
maximum unit strain energy computed for specimen W-29-14 was in
the order of 30,000 in-lbs per cu. in. This value is low when
compared with values of 90,000 to 100,000 in-lbs. per cu. in.
which may be expected at the crack.*

Several valuable observations may be made based upon a
study of how the plastic deformation propagates through inter-
mediate loadings up to and including maximum load. For this
purpose the 600 in-lb. per cubic inch contour was selected as
the boundary of plastic deformation areas (600 in-lb. per cu. in.
value selected on basis of general yielding as defined by the
uniaxial tests). Figure 35 gives the experimentally determined
areas enclosed by the 600 in-lbs. contours for all four quadrants
plotted against total observed energy input over the 9" gage
lengths. The plot gives values for the specimen W-29-3 and
W-29-4. The observations made on the basis of Figure 35 are:

1. The area enclosed by the 600 in-lb. contour appears
    to bear a linerar relation to the energy input for either
    specimen.

*Calculations based on theoretical strain energy conditions for
fracture give a value of 90,000 in-lbs. per cu in. The Univer-
sity of California has reported unit energy values in the order
of 150,000 in-lbs per cu. in. based on hardness surveys of the
fracture zone[5].
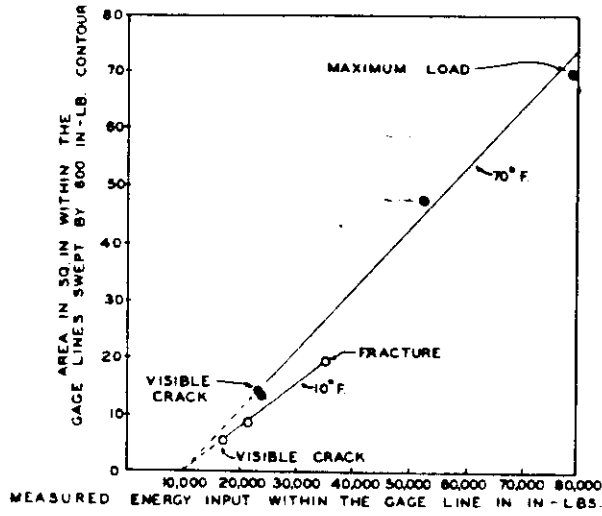
FIG. 35 MACRC-PROPAGATION OF PLASTIC DEFORMATION WITHIN 12" X 3/4" NOTCHED SPECIMENS UNDER LONGITUDINAL TENSION AT 70°F. AND 10°F.
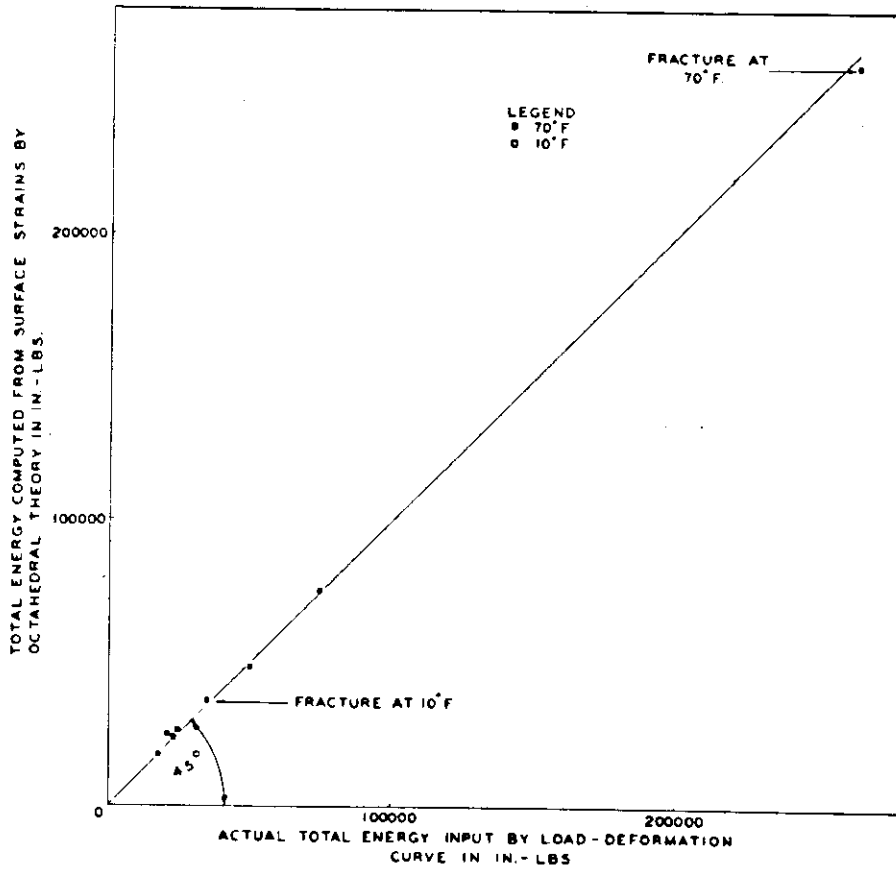
FIG 36 COMPARISON OF TOTAL STRAIN ENERGY BASED ON SURFACE STRAINS AND OCTAHEDRAL THEORY AGAINST ACTUAL TOTAL ENERGY INPUT

2. The volume of metal undergoing plastic deformation

appears to decrease with decreasing temperature.

Experimental Adjustments

Specimens W-29-3 and W-29-4 were unloaded at various loads, the grids measured and the specimens returned to the testing machine for reloading. This procedure necessitated that adjustments be made to the calculated strain energy based on the grid analysis. The calculated total strain energy was less than the actual energy input due to the fact that the measured surface strains for the unloaded specimen were less than those for the loaded specimen by the amount of elastic recovery. This adjustment was accomplished by adding to the total calculated strain energy an amount of energy determined from the observed load-deformation curve for the specimen.

The two effects of strain-aging, which occurred in the interim during grid measurements, were an increase in strength, and a decrease in ductility. A direct comparison between the total strain energy computed from grid measurements for specimens W-29-3 and W-29-4 and the total energy input determined by their load-elongation diagrams was impossible due to these effects. To provide a basis of comparison it was necessary to determine the load-elongation diagram of two additional specimens loaded continuously and tested at temperatures equivalent to the specimens under discussion. It was assumed that the energy obtained at equal deformations for the strain-aged specimens and the

unaffected specimens were comparable. The reason for taking equal elongations for comparison is that for the same amount of elongation, the values of local strains produced within the gage lines should be the same, no matter whether the specimen is strain-aged or not.

Figure 36 indicates the degree of correlation between the total energy computed from surface strains by the octahedral theory and the actual total energy input. The assumptions and adjustments previously discussed have been incorporated. The close correlation noted indicates that the assumptions and adjustments are substantially correct.

Correlation with Specimens of Varying Width and Constant Thickness

It appears that the total energy absorption of individual plates of various width, but of the same thickness (3/4"), can be predicted by using the energy distribution found in the 12" wide specimens. This is a possibility since it is believed that the energy at the notch and initial crack is the same regardless of width of specimen where failure occurs in the shear mode. Also at the end of an advancing crack, the natural notch acuity is essentially the same regardless of the width of the specimen.

The first step in examining this point of view consisted in superimposing, to scale, the outlines of one quadrant of plates of various widths upon the contour pattern for specimen W-29-4

shown in Figure 33. The superimposed quadrant of a plate of given width had a width equal to one-half of the actual width of the plate, and a length equal to one-half the gage length where the gage length was three-fourths of the width of the specimen, as in the 12" specimen. In superimposing this quadrant upon Figure 33 the ends of the notches were made coincident with the notch of the 12" wide plate as shown in Figure 37. The superimposed plates had aspect ratios varying from 1 to 13.3.

The plates so superimposed were compared by computing the average unit energy (in-lbs per cu. in) within the "gross gage volume" for maximum load by making use of the unit energy contours of specimen W-29-4 falling within the boundaries of the superimposed specimens. The average unit energy so computed is termed (u'). These derived values are plotted in Figure 38.

Independently of the foregoing procedure, the average unit energy (u) at maximum load for individual 3/4" thick ductile specimens of 3, 6, and 12" width were determined experimentally. These values of (u) are also shown in Figure 38 along with values of (u) for plates of greater width derived from data given in the final report[6] of the University of Illinois for "Dn" steel, which is somewhat similar to "W" steel. The dotted extension of the (u) curve must be considered as tentative and only indicative that 12" wide specimens may be useful in predicting the averaging unit energy for wider plates.
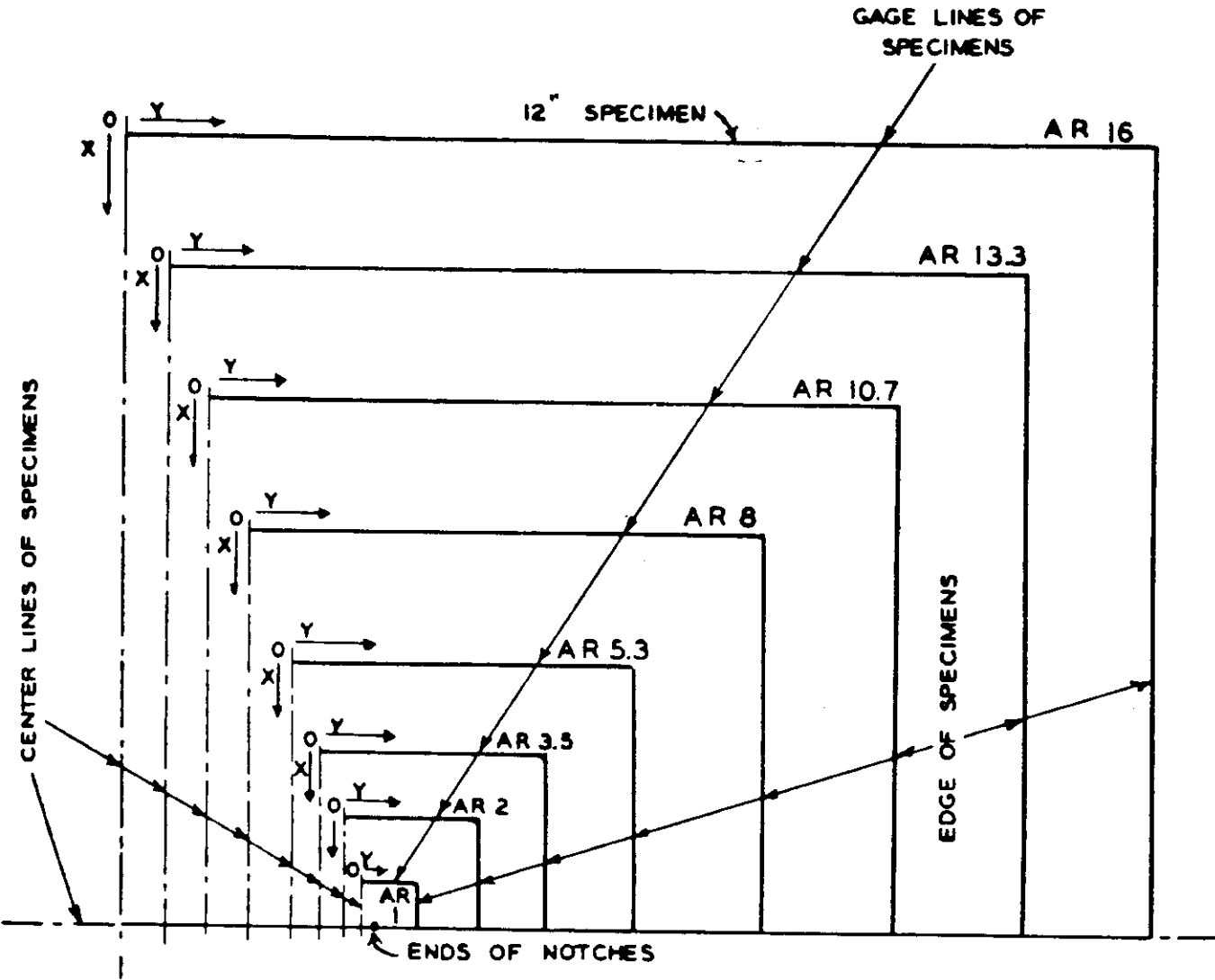
FIG. 37 QUARTER VIEW, SHOWING OUTLINES OF
SPECIMEN WITH TWO-DIMENSIONAL SIMILARITY
SUPERIMPOSED ON THE SURFACE OF A 12"
SPECIMEN, WITH ALL NOTCH ENDS COINCIDING
WITH EACH OTHER.

-68-

The differences between the (u') curve and (u) curve of Figure 38 may be attributed to strain aging. The (u) curve was determined from specimens continuously tested. This is largely confirmed by adjusting the experimental value of (u) for an aspect ratio of 16 to a value comparable to (u') by the medthods previously described. It was found that the adjusted value of (u), plotted as a hollow square in Figure 38, checked the (u') value obtained for W-29-4 in the presence of strain aging. This indicates a good possibility that the two curves (u) and (u') would coincide in the absence of strain aging.

These apparent correlations strongly suggest that the strain energy distribution of a single specimen of proper width and a given thickness may be used to predict the energy absorption of individual plates of varying width.

CONCLUSIONS - PART III

1. By use of the octahedral stress-strain function, energy distributions were plotted and typical patterns of plastic flow obtained.

2. Study of patterns of strain distribution is believed to be the key to successful prediction of service behavior from laboratory tests.

FIG. 38   CORRELATION BETWEEN THE UNIT STRAIN ENERGY DISTRIBUTION
IN A 12"x 3/4" NOTCHED SPECIMEN AND THE AVERAGE UNIT ENERGY
OF 3/4" THICK NOTCHED SPECIMENS, VARYING IN WIDTH.

ASPECT RATIO

U OR $U' =$ IN-LBS./CU.IN.

DIFFERENCE ATTRIBUTED
TO STRAIN AGING
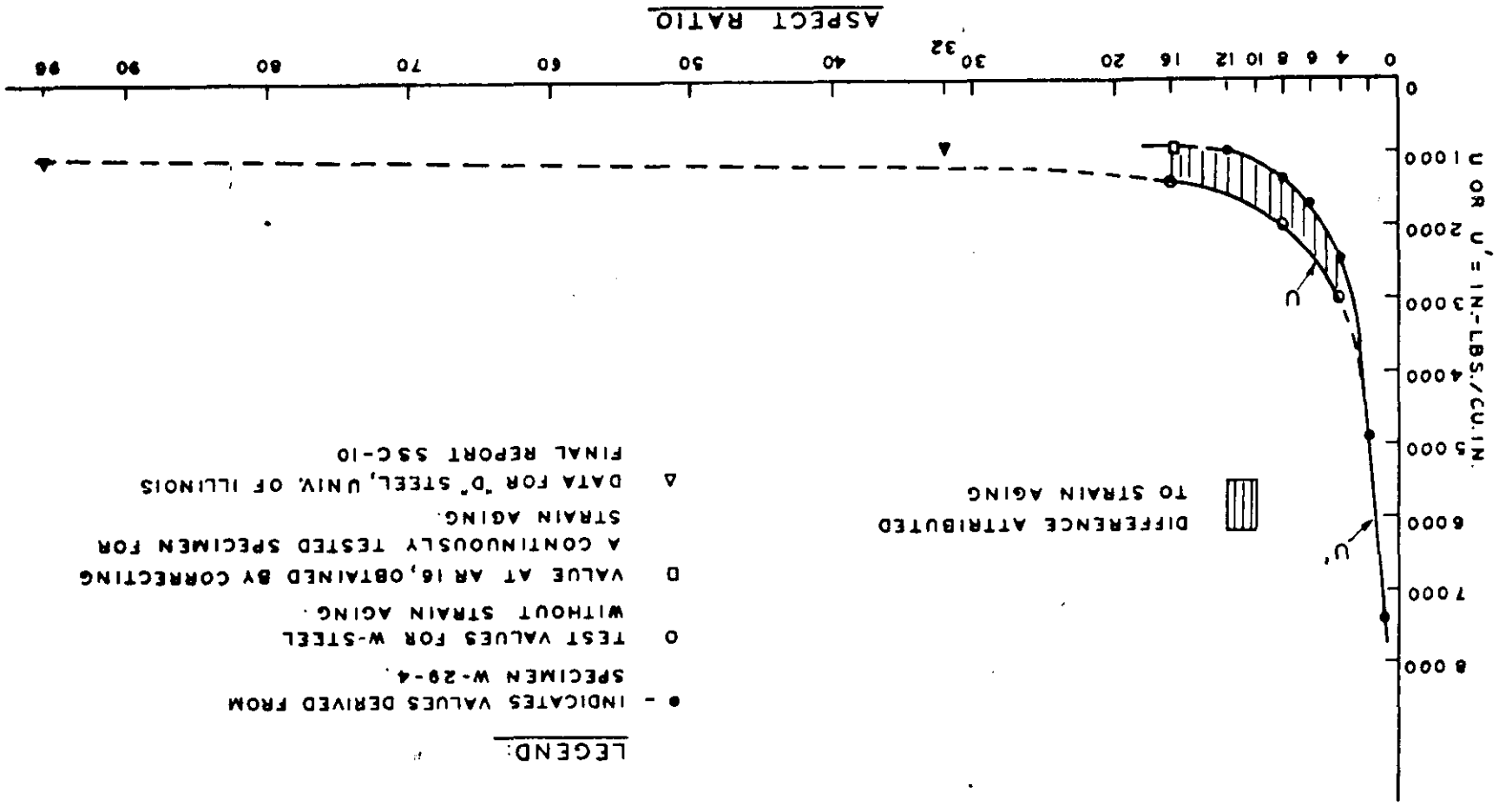
LEGEND:

● — INDICATES VALUES DERIVED FROM
SPECIMEN W-29-4.

○   TEST VALUES FOR W-STEEL
WITHOUT STRAIN AGING.

□   VALUE AT AR 16, OBTAINED BY CORRECTING
A CONTINUOUSLY TESTED SPECIMEN FOR
STRAIN AGING.

△   DATA FOR "D" STEEL, UNIV. OF ILLINOIS
FINAL REPORT SSC-10

ACKNOWLEDGMENTS

Revision Nov. 30, 1951

BIBLIOGRAPHY

1. S. T. Carpenter, W. P. Roop, N. Barr, E. Kasten and
    A. W. Zell, Swarthmore College, "Twelve Inch Wide Flat
    Plate Tests", Progress Report, Ship Structure Committee,
    Serial No. SSC-21, April, 1949.

2. S. T. Carpenter, W. P. Roop, E. Kasten and A. W. Zell,
    Swarthmore College, "Twelve Inch Wide Flat Plate Tests
    and Aspect Ratio Program", Progress Report, Ship Structure
    Committee, Serial No. SSC-35, December, 1949.

3. S. T. Carpenter, W. P. Roop, A. W. Zell, E. Kasten,
    Swarthmore College, "The Effects of Width and Thickness
    on Strength, Energy Absorption and Transition Temperature
    for Internally Notched Flat Steel Plates", Progress Report,
    Ship Structure-Committee, Serial No. SSC-44, November, 1951.

4. S. I. Liu and S. T. Carpenter, Swarthmore College, "A Study
    of Plastic Deformation and Fracturing by Strain Energy
    Distribution", Progress Report, Ship Structure Committee,
    Serial No. SSC-38, December, 1950.

5. H. E. Davis, G. E. Troxel, E. R. Parker, A. Boodberg, M. P.
    O'Brien, University of California, "Causes of Cleavage
    Fracture in Ship Plate Flat Plate Tests and Additional
    Tests on Large Tubes", Final Report, Ship Structure Committee,
    Serial No. SSC-8, January, 1947.

6. W. M. Wilson, R. A. Hechtman, and W. H. Bruckner, University
    of Illinois, "Cleavage Fracture of Ship Plates as Influenced
    by Size Effect", Final Report, Ship Structure Committee,
    Serial No. SSC-10, June, 1947.

7. E. M. McCutcheon, C. L. Pittiglio and R. H. Raring,
    "Transition Temperature of Ship Plate in Notched Tensile
    Tests", The Welding Journal, vol. 29, No. 4, 1950 Research
    Supplement, pages 184S-194S.

8. N. A. Kahn and E. A. Imbembo, "A Method of Evaluating Transi-
    tion from Shear to Cleavage Failure in Ship Plate and its
    Correlation with Large-Scale Plate Tests", The Welding Journal
    Research Supplement, vol. 27, 1948, pages 169-S - 184-S

BIBLIOGRAPHY (Cont'd)

9. N. A. Kahn and E. A. Imbembo, "Further Study of Navy Tear Test", The Welding Journal Research Supplement, February, 1950.

10. E. R. Parker, "The Effect of Section Size on the Fracture Strength of Mild Steel", in Fracturing of Metals, American Society for Metals, 1948.

11. P. E. Shearin, A. E. Ruark, and R. M. Trimble, "Size Effects in Steels and Other Metals from Slow Notch Bend Tests", in Fracturing of Metals, American Society for Metals, 1948.

12. F. Fettweis, "Die Kerbschlagprobe. Entwicklung und Kritik" ("The Notch Impact Test-Development and Criticism"), Archiv für das Eisenhüttenwessen, 2 (1929) pp 625-674. Translated by L. Emmerich and E. P. Klier and distributed by the Ship Structure Committee, April, 1951.

13. Wendell P. Roop, Discussion of Paper by Harry C. Boardman, (p. 295-s) and by Rosenthal and Mitchell (p. 319-s) in Welding Research Supplemtn, June, 1951.

14. R. H. Raring, "Load Deflection Relationships in Slow Bend Tests of Charpy V-Notch Specimens"; American Society for Testing Materials, 1952 Preprint 65, Presented at 1952 Annual Meeting.

APPENDIX

TABLE I

CHEMICAL COMPOSITION

Steel Code	C%	Mn%	P%	S%	Si%	Al%	Ni%	Cu%	Cr%	Mo%	N%	Type Steel
A	.26	.50	.012	.039	.03	.012	.02	.03	.03	.006	.004	semi-killed
Bn	.18	.73	.011	.030	.04	.013	.06	.08	.03	.006	.006	semi-killed normalized
Br	.18	.75	.008	.030	.07	.015	.05	.07	.03	.006	.005	semi-killed
C	.24	.48	.012	.026	.05	.016	.02	.03	.03	.005	.009	semi-killed
Dn	.19	.54	.011	.024	.19	.019	.15	.22	.12	.021	.006	fully-killed normalized
E	.20	.33	.013	.020	.01	.009	.15	.18	.09	.018	.005	rimmed
W	.20	.52	.013	.010	.23	.006	.10	.16	.07	.01	.005	fully-killed
S-9	.21	.50	.012	.020	.07	.002	.07	.02	.05	.004	.004	semi-killed
S-12	.20	.82	.011	.030	.07	.04	.03	.05	.04	.01	.004	semi-killed fine grained*
S-22	.21	.82	.012	.020	.09	.006	.03	.05	.04	.01	.004	semi-killed coarse grained**

* Aluminum added in Ladle and in Mold

**   "   "   " Ladle only

TABLE 2

PHYSICAL PROPERTIES

Unnotched bars - Swarthmore Tests
A.S.T.M. Standard Specimens

Steel Code	Yield Stress p.s.i.	Ultimate Tensile Strength p.s.i.
A	31,400	59,500
Bn	32,100	59,300
Br	32,200	57,700
C	37,400	67,800
Dn	34,300	61,300
E	33,200	59,200
W	37,230	62,540
S-9	32,600	57,900
S-12	34,700	64,100
S-22	35,000	63,800

TABLE 3

"A" Steel

TESTS OF SPECIMENS 12" WIDE, 3/4" THICK WITH STANDARD NOTCH

(The notch is 3" wide and has at its extremities a cut 1/8" long and 0.010" wide made with a jeweler's hack-saw)

Spec. No.	Temperature °F	Visible Crack Energy in-lbs.	Load lbs.	Max. Load Energy in-lbs.	Load lbs.	Failure Energy in-lbs.	Load lbs.	Type of Failure % Shear
A-18-13	31	6,500	247,500	13,800	248,500	13,800	248,500	0
A-19-11	38	1,100	230,000	29,300	283,000	29,300	283,000	0
A-19-2	38	5,300	240,500	22,800	265,400	22,800	265,400	0
A-19-3	38	6,400	245,000	61,600	312,500	61,600	312,500	10
A-18-5	40	4,200	241,000	21,900	270,300	21,900	270,300	0
A-19-1	42	4,000	230,000	95,900	321,600	234,500	60,000	100
A-19-0	43	2,800	230,000	22,400	265,500	22,400	265,500	0
A-19-4	46	1,100	230,000	24,400	256,000	24,400	256,000	0
A-19-12	46	1,200	230,000	117,300	328,000	249,200	131,000	100
A-18-17	48	10,300	235,500	43,100	283,000	43,100	283,000	0
A-18-15	50	11,200	248,000	100,900	319,500	240,900	80,000	100
A-18-6	51	7,800	241,500	91,500	322,000	236,300	67,000	100
A-18-14	52	4,000	234,500	20,700	265,000	20,700	265,000	0
A-18-20	58	8,500	240,000	31,000	274,000	31,200	274,000	0
A-18-7	58	14,100	250,000	92,400	319,500	233,900	68,000*	100
A-18-16	58	8,300	235,000	100,500	319,000	250,600	72,000*	100
A-18-8	59	11,700	243,700	91,100	318,000	232,100	52,000*	100
A-18-11	66	18,700	253,000	104,600	315,000	229,400	58,000	100
A-18-3	66	12,300	243,000	92,800	314,300	234,000	50,000	100
A-18-12	71	17,100	250,000	86,400	314,400	247,100	95,000	100
A-18-18	71	16,600	250,000	104,300	317,000	263,700	15,000	100
A-18-4	71	10,100	243,000	84,700	312,500	232,700	76,500	100
A-18-19	82	10,900	237,600	99,700	314,000	274,000	90,000	100
A-18-1	88	12,600	238,000	82,400	312,200	237,900	50,000	100
A-18-9	88	11,300	240,000	98,100	314,500	255,600	50,000	100
A-18-10	97	15,300	248,500	93,000	314,500	230,200	50,000	100
A-18-2	97	12,400	238,000	92,600	311,500	263,700	50,000	100

* Indicates that this was not the load at fracture, but is given as the last load immediately preceding fracture.

TABLE 4

"B$_N$" Steel

TESTS OF SPECIMENS 12" WIDE, 3/4" THICK WITH STANDARD NOTCH

(The notch is 3" wide and has at its extremities a cut 1/8" long and 0.010" wide made with a jeweler's hack-saw)

Spec. No.	Temp. °F	Visible Crack Energy in-lbs.	Load lbs.	First Maximum Energy in-lbs.	Load lbs.	Second Max. Energy in-lbs.	Load lbs.	Failure Energy in-lbs.	Load lbs.	Type of Failure % Shear
B$_N$-21-7	-8.9	4,700	238,000	41,500	272,000	-	-	41,500	272,000	0
B$_N$-21-1	-1.2	7,700	240,000	32,900	270,800	-	-	32,900	270,800	0
B$_N$-21-8	1.2	6,300	242,000	41,300	283,400	44,500	279,400	44,500	279,400	1
B$_N$-21-2	9.1	6,400	238,700	59,700	295,700	-	-	59,700	290,000	3
B$_N$-21-9	9.2	7,700	240,500	53,900	289,300	-	-	53,900	289,300	3
B$_N$-21-18	9.9	4,900	243,400	30,000	274,000	-	-	30,000	274,000	0
B$_N$-21-6	10.0	4,000	240,000	137,000	326,300	-	-	309,100	50,000	100
B$_N$-21-14	10.0	4,600	245,400	49,200	292,500	51,000	288,000	57,000	288,000	2
B$_N$-21-10	18.9	5,200	236,300	70,200	309,000	-	-	70,200	309,000	3
B$_N$-21-3	19.8	6,500	234,800	125,600	321,800	-	-	266,700	199,000	66
B$_N$-21-4	23.8	3,300	227,500	56,100	299,400	-	-	56,100	299,400	3
B$_N$-21-11	24.5	6,400	234,800	60,600	294,700	-	-	60,600	294,700	3
B$_N$-21-15	25.3	5,900	233,800	29,800	263,500	-	-	29,800	263,500	1
B$_N$-21-12	29.4	6,400	234,500	121,500	318,900	-	-	293,500	25,000	100
B$_N$-21-17	29.8	5,700	234,900	120,000	317,700	-	-	290,400	50,000	100
B$_N$-21-16	29.9	4,700	237,600	118,200	320,400	-	-	295,600	22,000	100
B$_N$-21-20	30.2	4,900	235,500	119,000	324,800	-	-	294,000	40,000	100
B$_N$-21-19	41.3	3,400	229,800	123,500	316,000	-	-	287,200	30,000	100
B$_N$-21-5	73.8	3,800	222,500	115,000	310,000	-	-	292,500	41,000	100

TABLE 5

"B$_R$" Steel

TESTS OF SPECIMENS 12" WIDE, 3/2" THICK WITH STANDARD NOTCH

(The notch is 3" wide and has at its extremities a cut 1/8" long and 0.010" wide made with a jeweler's hack-saw)

Spec. No.	Temperature °F	Visible Crack		Max. Load		Failure		Type of Failure % Shear
		Energy in-lbs.	Load lbs.	Energy in-lbs.	Load lbs.	Energy in-lbs.	Load lbs.	
B$_R$-22-18	-12.7	3,900	234,200	36,700	293,000	36,700	293,000	1
B$_R$-22-8	-10.3	6,700	249,300	31,500	283,500	31,500	280,000	0
B$_R$-22-9	1.9	9,900	245,000	46,700	296,300	46,800	295,000	2
B$_R$-22-11	2.0	4,800	240,800	92,640	332,500	92,600	328,000	6
B$_R$-22-17	2.8	1,600	224,800	36,000	290,000	36,000	290,000	1
B$_R$-22-10	11.6	10,100	240,500	143,300	340,100	335,100	74,500	100
B$_R$-22-5	11.9	7,800	243,300	138,600	346,500	286,800	210,000	59
B$_R$-22-2	12.1	10,500	239,500	34,300	279,500	34,300	279,500	0
B$_R$-22-12	13.0	5,200	232,200	134,000	329,700	310,900	32,000	100
B$_R$-22-7	13.6	6,300	237,300	30,000	280,500	30,000	280,500	1
B$_R$-23-20	19.3	3,400	230,000	120,000	325,600	295,100	78,000	100
B$_R$-22-19	19.6	3,500	230,000	120,000	329,300	306,500	40,000	100
B$_R$-22-4	20.3	2,700	230,000	120,000	329,500	315,500	45,000	100
B$_R$-22-3	30.0	1,000	224,500	129,200	329,500	316,300	35,000	100
B$_R$-22-1	41.5	7,400	230,700	132,900	337,300	330,400	25,000	100
B$_R$-22-6	68.8	6,500	228,500	140,200	327,000	350,800	30,000	100

TABLE 6

"C" Steel

TESTS OF SPECIMENS 12" WIDE, 3/4" THICK WITH STANDARD NOTCH

(The notch is 3" wide and has at its extremities a cut 1/8" long and 0.010" wide made with a jeweler's hack-saw)

Spec. No.	Temperature °F	Visible Crack		Max. Load		Failure		Type of Failure % Shear
		Energy in-lbs.	Load lbs.	Energy in-lbs.	Load lbs.	Energy in-lbs.	Load lbs.	
C-24-7	63	1,700	256,300	18,600	287,500	18,600	287,500	0
C-24-19	63	15,100	273,000	32,600	281,000	32,600	252,000	0
C-24-14	73	15,100	275,000	29,200	316,000	29,200	316,000	0
C-24-17	73	40,400	286,000	40,400	286,000	140,100	72,500	65
C-24-5	74	2,000	227,700	42,000	291,700	151,400	60,000	59
C-24-13	78	12,100	267,500	40,500	295,000	40,500	295,000	0
C-24-8	81	4,300	261,500	97,600	308,300	114,600	298,000	15
C-24-20	82	15,700	276,000	42,800	291,200	57,100	236,800	0
C-24-6	88	4,500	255,500	55,200	310,700	137,100	147,000	40
C-24-15	88	15,900	275,500	49,700	293,000	49,700	293,000	0
C-24-18	89	33,400	292,000	33,400	292,000	45,200	278,700	0
C-24-10	96	22,500	287,500	60,700	311,500	147,300	54,000	58
C-24-2	97	1,900	248,500	87,300	308,500	205,300	17,000	71
C-24-9	107	15,500	271,000	91,200	321,500	278,800	75,000	89
C-24-1	108	3,900	249,000	128,900	370,000	268,900	216,400	63
C-24-3	116	5,800	254,500	130,600	360,000	238,300	50,000	100
C-24-11	116	30,100	300,000	117,000	371,500	329,200	60,000	100
C-24-4	124	10,100	262,500	104,200	369,000	299,400	80,000	100
C-24-12	124	8,500	250,000	95,300	344,100	236,700	59,000	92
C-24-16	130	14,200	275,000	91,300	374,000	291,200	100,000	100

TABLE 9

Code S-9 (A.S.T.M. Steel)

Test specimens 12" wide x 3/4" thick, with standard notch

The notch is 3" wide and has at its extremities a cut 1/8" deep made with a .010" Jeweler's hacksaw

Spec. No.	Deg. F	To Visible Crack Energy E in lbs	Load lbs.	To Maximum Load Energy E_1 in lbs.	Load lbs.	To Failure Energy E_2 in lbs	Load lbs.	Energy $E_2 - E_1$ in lbs.	% Shear
11	92	13,600	229,600	118,200	326,600	310,100	20,000	191,900	100
16	74	9,800	229,600	105,800	278,000	256,500	19,500	150,700	75
10	70	12,000	231,800	151,800	338,500	311,100	30,000	159,300	100
12	60	12,000	233,000	130,900	336,500	333,600	51,000	202,700	100
18	60	11,500	229,000	54,200	295,600	54,200	295,600	0	0
1	50	12,500	236,000	121,400	334,000	309,000	70,000	187,600	100
6	50	9,500	227,500	125,000	336,300	325,000	49,000	200,000	100
7	45	9,100	234,000	43,000	287,000	43,000	287,000	0	0
3	40	11,000	236,800	41,200	288,800	41,200	288,800	0	0

TABLE 10

Code S-9 (A.S.T.M. Steel)

Test specimens 12" wide x 3/4" thick, with standard notch

The notch is 3" wide and has at its extremities a cut 1/8" deep made with a .010" Jeweler's hacksaw

Spec. No.	Deg. F	To Visible Crack Energy E in.lbs	Load lbs.	To Maximum Load Energy E_1 in.lbs	Load lbs.	To Failure Energy E_2 in.lbs.	Load lbs.	Energy $E_2 - E_1$ in.lbs.	% Shear
1	78	10,000	250,000	114,000	356,000	294,000	45,000	180,000	100
8	40	8,000	258,200	110,000	363,000	290,000	55,000	180,000	100
15	30	5,000	235,500	128,000	366,400	300,000	77,000	172,000	100
3	20	10,000	254,400	111,000	365,800	286,500	150,000	175,500	70
12	15	4,000	248,000	102,000	366,700	296,000	45,000	194,000	100
2	9	7,000	253,000	97,000	366,500	97,000	366,500	0	10
7	7	7,000	267,000	39,000	326,000	39,000	326,000	0	0
9	0	6,300	243,000	112,000	371,000	214,000	320,000	102,000	30
10	0	2,500	250,000	98,500	378,000	98,500	378,000	0	5
5	-10	9,000	268,500	108,000	375,000	220,000	305,000	112,000	30
11	-20	5,000	259,000	90,200	375,600	90,200	375,600	0	8
14	-30	7,200	263,500	86,900	376,300	86,900	376,300	0	8

TABLE 11

Code S-22 (Coarse grain)

Test specimens 12" wide x 3/4" thick, with standard notch

The notch is 3" wide and has at its extremities a cut 1/8" deep made with a .010" Jeweler's hacksaw

Spec. No.	Deg. F	To Visible Crack Energy E in.lbs.	Load lbs.	To Maximum Load Energy E_1 in.lbs.	Load lbs.	To Failure Energy E_2 in.lbs.	Load lbs.	Energy $E_2 - E_1$ in.lbs.	% Shear
3	70	5,600	247,800	127,900	375,000	330,000	53,000	202,100	100
8	60	2,500	234,000	104,800	376,500	334,000	40,000	229,200	100
10	60	7,500	253,500	130,500	375,900	212,000	320,000	81,500	35
9	54	7,500	261,000	35,000	312,000	210,000	312,000	175,000	22
7	50	5,400	252,200	35,600	330,000	35,600	330,000	0	0
1	40	5,300	242,500	43,800	332,000	43,800	332,000	0	0
15	20	12,700	265,000	29,000	308,500	29,000	308,500	0	5

TABLE 12

"W" Steel

TESTS OF SPECIMENS 12" WIDE, 3/4" THICK WITH STANDARD NOTCH

(The notch is 3" wide and has at its extremities a cut 1/8" long and 0.010" wide made with a jeweler's hack saw)

Spec. No.	Temperature °F	Visible Crack Energy E in-lbs.	Load lbs.	Max. Load Energy E_1 in-lbs.	Load lbs.	Failure Energy E_2 in-lbs.	Load lbs.	Type of Failure % Shear
W-32-11	21	4,000	257,800	48,000	309,300	48,000	309,300	0
W-32-12	36	3,500	253,000	67,500	346,000	71,000	340,600	22
W-32-9	43	5,300	250,800	40,000	306,000	40,000	306,000	0
W-32-10	45	8,700	256,000	120,000	345,700	158,000	330,000	30
W-32-15	50	5,000	253,600	125,500	345,500	300,200	22,000	100
W-32-8	54	4,500	257,000	107,500	346,800	292,300	30,500	100
W-32-2	66	not obtained		93,000	335,000	253,000	150,000	100
W-32-6	66	3,500	228,300	142,600	340,700	not obtained		100
W-33-16	71	25,100	276,500	129,720	338,500	317,000	126,000	100
W-32-17	76	19,700	260,000	109,700	310,000	244,800	61,000	100
W-32-1	81	not obtained		102,700	345,000	263,600	71,500	100
W-32-7	81	8,000	250,000	110,000	342,100	232,500	55,000	100

TABLE 13

Comparisons of Maximum Loads for Shear and Cleavage Fracture

(Net area before test, 6.75 in^2.)

Steel Code	Column 1 Average Max. Load in lbs. specimens failing in 100% shear	Column 2 Average Max. Load in lbs. specimens failing in 0% shear	Ratio of Column 1 to Column 2
A	317,000	268,000	1.18
Br	333,000	288,000	1.16
Bn	319,000	286,000	1.11
C	348,000	294,000	1.18
Dn	346,000	311,000	1.11
E	318,000	264,000	1.20
W	338,000	307,600	1.10
S-9	337,200	290,500	1.16
S-12	362,000	326,000	1.11
S-22	375,800	331,000	1.13

TABLE 14

Comparison of Energy Absorbed to Maximum Load for Shear and Cleavage Fractures

Steel Code	Column I Average Energy Specimens Failing in 100% Shear in.lbs.	Column 2 Average Energy Specimens Failing in 0% Shear in.lbs.	Ratio of Column 1 to Column 2
A	95,700	25,500	3.75
Br	131,000	34,300	3.80
Bn	122,000	47,800	2.56
C	105,000	38,400	2.74
Dn	128,000	49,200	2.60
E	99,800	32,000	3.12
W	127,600	44,000	2.90
S-9	129,500	46,100	2.81
S-12	113,500	*	
S-22	116,400	39,700	2.92

*   (No specimens tested exhibited 0% shear)

TABLE 15

SUMMARY of TRANSITION TEMPERATURES 12" wide PLATES
(Degrees Fahrenheit)

12" Wide Tests

Steel Code	SWARTHMORE DATA				University of Illinois[6]	University of California[5]	Transition temp. by Navy Tear Test[8]
	Transition Temp. Range		Single Value of Transition Temp. at Mid Point Transition Curve				
	Based on Energy to max. load	Based on Appearance of Fracture	Based on Energy to max. load	Based on Appearance of Fracture			
A	50° to 60°	50° to 60°	42°	41°	----	25°	70°
Br	10° to 20°	10° to 20°	9°	11°	----	5°	60°
Bn	25° to 30°	25° to 30°	26°	27°	----	15°	----
C	90° to 105°	110° to 125°	95°	94°	----	90°	135°
Dn	20° to 25°	20° to 25°	18°	19°	0° to 30°	----	70°
E	90° to 105°	90° to 105°	85°	77°	80° to 120°	----	140°
W	40° to 50°	40° to 50°	44°	46°	----	----	60°
S-9	50° to 60°	50° to 75°	48°	58°	----	----	80°
S-12	indefinite	10° to 30°	20°?	12°	----	----	40°
S-22	50° to 60°	50° to 60°	57°	57°	----	----	100°

TABLE 16

Transition Temperature as affected by Mn/C Ratio

Steel Code	Mn/C ratio	Order of low to High Mn/C ratio	Order of high to low of Trans. Temp. based on range
A	1.92	2	7
Br	4.16	10	10
Bn	4.05	9	6
C	2.00	3	1
Dn	2.84	6	8
E	1.65	1	2
W	2.48	4	5
S-9	2.78	5	4
S-12	3.50		9
S-22	3.50	(7,8)	3

TABLE 17

Physical Properties

Unnotched Bars
ASTM Standard

Steel Code	Plate Thickness	Yield Stress psi	Ultimate Stress psi
T-1	1/2"	41,000	67,200
	3/4"	35,800	63,200
	1"	37,200	71,000
T-2	1-1/2"	36,400	60,000
	3/4"	39,600	67,000
	1"	40,000	67,000
T-2R	1-1/2"	33,800	64,500
	3/4"	39,200	67,000

TABLE 18

Aspect Ratios Tested

Steel Code	Thickness	Aspect Ratios
T-1	1/2"	4,8,16,19.5
	3/4"	4,8,12,16
	1"	4,8,12
T-2	1-1/2"	4,6
	3/4"	4,8,12,16
	1"	4,6,8,12
T-2R	1-1/2"	4,6
	3/4"	4,6,16,19.5

TABLE 19

T-1 STEEL

Summary of Unit Energy* and Average Unit Stress at Maximum Load

Values Based on Gross Gage Volume and Net Area

and the average for all specimens exhibiting either 100% or 0% shear failures

Thickness	Percent of Shear	AR 4 u	psi	AR 6 u	psi	AR 8 u	psi	AR 12 u	psi	AR 16 u	psi	AR 19 u	psi
1/2"	100%	4,480	71,000			2,610	63,050			1,870	58,100	1,700	54,730
	0%	4,520	71,900			2,400	63,570			1,220	56,300	910	52,940
3/4"	100%	3,720	67,940			2,460	59,940	1,820	57,000	1,610	55,080		
	0%	3,810	69,230			2,000	59,530	1,420	56,460	1,350	53,620		
1"	100%	3,090	61,720			2,330	55,420	1,860	52,550				
	0%	3,190	62,680			1,900	57,160	1,245	52,680				
1 1/2"	100%	2,800	59,130	2,250	56,300								
	0%	2,540	60,200	1,960	56,780								

* u, unit energy in inch-lbs. per cubic inch

-83-

TABLE 20

T-2 and T-2R STEELS

Summary of Unit Energy* and Average Unit Stress at Maximum Load

Values Based on Gross Gage Volume and Net Area

and the average of all specimens exhibiting either 100% or 0% shear failures

Thickness	Percent of Shear	AR 4 u	psi	AR 6 u	psi	AR 8 u	psi	AR 12 u	psi	AR 16 u	psi	AR 20 u	psi
						T-2 Steel							
3/4"	100%	3,350	66,820			2,160	60,770	1,600	57,600	1,530	55,360		
	0%	2,870	68,150			1,410	59,000	1,090	56,900	890	54,200		
1"	100%	2,160	63,130	1,970	60,200	1,770	56,500	1,460	54,500				
	0%	2,750	63,830	—	—	1,660	59,000	970	54,890				
1 1/2"	100%	2,270	59,770	1,920	58,000								
	0%	2,270	61,250	1,570	57,530								
						T-2R Steel							
3/4"	100%	2,970	63,630	2,750	61,360					1,550	55,000	1,340	53,800
										770	52,800	—	—

* u, unit energy in inch-lbs. per cubic inch.

TABLE 21

TRANSITION TEMPERATURES

T-1 STEEL

Plate Thickness	Aspect Ratio	Transition Temperature Range °F Based on appearance of fracture as defined by % of shear	Single Point Transition Temp. °F based on appearance as defined by % of shear
1/2"	4	-20 to zero	-10
	8	-10 to zero	-10
	16	+10 to 20	- 2
	19	-10 to zero	- 8
3/4"	4	-20 to zero	-23
	8	zero to +10	zero
	12	zero to +10	+ 5
	16	+30 to 40	+15
1"	4	+10 to +20	+13
	8	+10 to +20	+13
	12	+30 to +40	+28
1 1/2"	4	+50 to 60	+44
	6	50 to 60	+50

TABLE 22

TRANSITION TEMPERATURES

T-2 and T-2R STEELS

| Plate Thickness | Aspect Ratio | Transition Temperature Range °F | Single Point |
		Based on appearance of fracture as defined by % of shear	Transition Temp. °F based on appearance as defined by % of shear
		T-2 Steel	
3/4"	4	-20 to -10	-17
	8	-10 to - 5	-18
	12	-10 to zero	- 5
	16	+10 to +20	+ 2
1"	4	-10 to zero	- 7
	6	+10 to +20	+10
	8	+30 to +40	+33
	12	zero to +20	+13
1 1/2"	4	+30 to +40	+30
	6	+60 to +75	+68
		T-2R Steel	
3/4"	4	(Insufficient Data)	
	6	(Insufficient Data)	
	16	+40 to +50	+38
	20	+35 to +50	+38